New Insights into the South American Low-Level Jet from RELAMPAGO Observations

CLAYTON R. S. SASAKI,[a] ANGELA K. ROWE,[b] LYNN A. MCMURDIE,[a] AND KRISTEN L. RASMUSSEN[c]

[a] *Department of Atmospheric Sciences, University of Washington, Seattle, Washington*
[b] *Department of Atmospheric and Oceanic Sciences, University of Wisconsin–Madison, Madison, Wisconsin*
[c] *Department of Atmospheric Science, Colorado State University, Fort Collins, Colorado*

(Manuscript received 27 June 2021, in final form 4 February 2022)

ABSTRACT: The Remote sensing of Electrification, Lightning, And Mesoscale/microscale Processes with Adaptive Ground Observations (RELAMPAGO) campaign produced unparalleled observations of the South American low-level jet (SALLJ) in central Argentina with high temporal observations located in the path of the jet and upstream of rapidly growing convection. The vertical and temporal structure of the jet is characterized using 3-hourly soundings launched at two fixed sites near the Sierras de Córdoba (SDC), along with high-resolution reanalysis data. Objective SALLJ identification criteria are applied to each sounding to determine the presence, timing, and vertical characteristics of the jet. The observations largely confirm prior results showing that SALLJs most frequently come from the north, occur overnight, and peak in the low levels, though SALLJs notably peaked higher near the end of longer-duration events during RELAMPAGO. This study categorizes SALLJs into shorter-duration events with jet cores peaking overnight in the low levels and longer 5–6-day events with elevated jets near the end of the period that lack a clear diurnal cycle. Evidence of both boundary layer processes and large-scale forcing were observed during shorter-duration events, whereas synoptic forcing dominated the longer 5–6-day events. The highest amounts of moisture and larger convective coverage east of the SDC occurred near the end of the 5–6-day SALLJ events.

SIGNIFICANCE STATEMENT: The South American low-level jet (SALLJ) is an area of enhanced northerly winds that likely contributes to long-lived, widespread thunderstorms in Southeastern South America (SESA). This study uses observations from a recent SESA field project to improve understanding of the variability of the SALLJ and the underlying processes. We related jet occurrence to upper-level environmental patterns and differences in the progression speed of those patterns to varying durations of the jet. Longer-duration jets were more elevated, transported moisture southward from the Amazon, and coincided with the most widespread storms. These findings enable future research to study the role of the SALLJ in the life cycle of storms in detail, leading to improved storm prediction in SESA.

KEYWORDS: South America; Jets; Convective storms; Radiosonde/rawinsonde observations; Wind; Reanalysis data; Mesoscale processes

1. Introduction

Some of the most intense convective storms in the world are located east of the Andes in central Argentina (Zipser et al. 2006; Houze et al. 2015; Liu and Zipser 2015) and growth into large, organized convection is frequent (Velasco and Fritsch 1987). Convective systems in this region have a duality of impacts. They provide the water supply that supports the population as well as the extensive agriculture industry, including major wine-producing regions, and produce greater than 90% of the rain in southeastern South America (Nesbitt et al. 2006; Rasmussen et al. 2016). Yet, at the same time, large hail, flooding rains, and frequent lightning create a major hazard for the people and crops in the region (Zipser et al. 2006; Matsudo and Salio 2011; Mezher et al. 2012; Rasmussen et al. 2014). Understanding how storms organize and grow into larger mesoscale systems can help with prediction of these high-impact weather events.

Previous modeling and satellite studies in central Argentina have emphasized the South American low-level jet (SALLJ) as a recurring feature around the time of development of mesoscale convective systems (MCSs; Nicolini and Saulo 2000; Salio et al. 2002; Salio et al. 2007; Borque et al. 2010; Rasmussen and Houze 2016). The SALLJ is a ribbon of fast-moving air in the lower levels of the atmosphere, oriented mostly north–south, that lies east of the Andes (blue arrow in Fig. 1) and transports warm, moisture-laden air from the tropics to the midlatitudes (Rasmusson and Mo 1996; Nogués-Paegle and Mo 1997; Vera et al. 2006; Nascimento

Corresponding author: Clayton R. S. Sasaki, crs236@uw.edu

DOI: 10.1175/MWR-D-21-0161.1

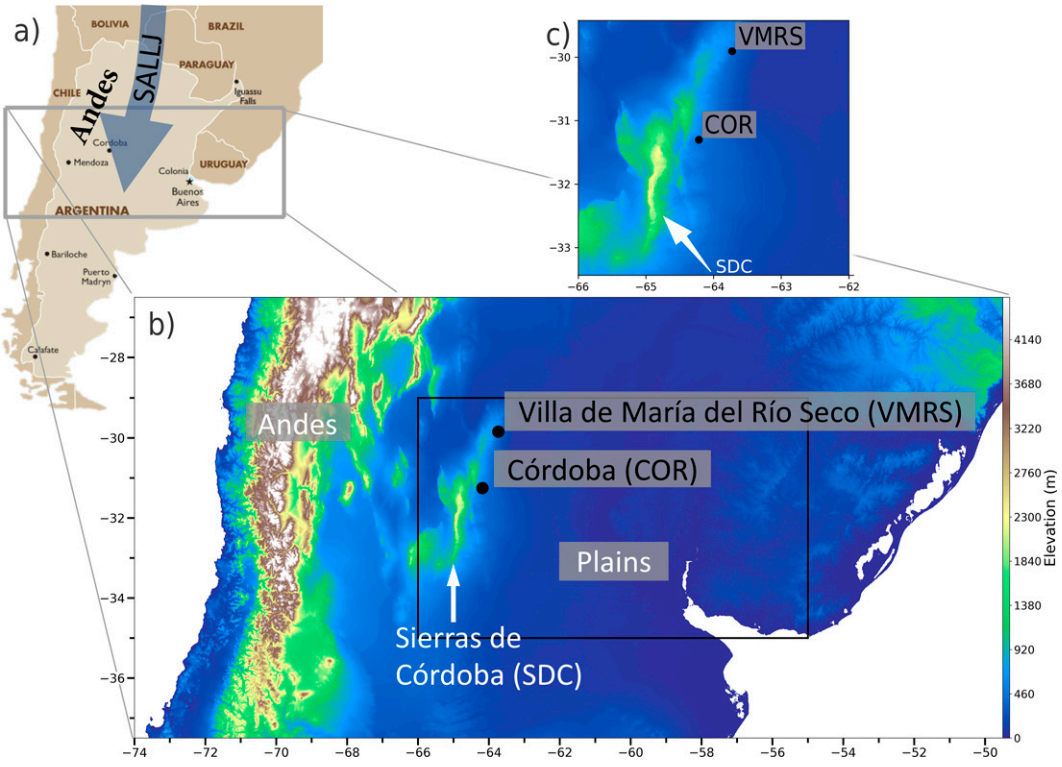

FIG. 1. Maps depicting the general RELAMPAGO study area: (a) map of southern South America with the SALLJ (blue arrow) highlighted; (b) zoomed-in map of the study area including the region of frequent growth of convection (black outline; used for *GOES-16* analysis), two fixed sounding sites (black text), and elevation (color shading) with notable topographic features for this study (white text); (c) zoomed-in map of the SDC topography near the two sites.

et al. 2016). Additionally, it has been hypothesized that when the SALLJ extends into central Argentina it creates favorable thermodynamic and dynamic conditions for convection beyond moistening the environment. These influences include increasing low-level convergence, wind shear, and persistent horizontal advection of heat (Salio et al. 2007; Saulo et al. 2007; Piersante et al. 2021). Detailed knowledge of the characteristics and variability of the SALLJ are needed to further our understanding of the relationship between the SALLJ and MCSs, which could be critical to predicting MCS development and maintenance (Carril et al. 2012; Anabor et al. 2008).

Past work, largely from a U.S. perspective, has linked low-level jets (LLJs) to many atmospheric mechanisms, but broadly classified them into two types: nocturnal and synoptically related LLJs (e.g., Stensrud 1996). Nocturnal LLJs (NLLJs) are associated with boundary layer processes such as inertial oscillations (Blackadar 1957), shallow baroclinic processes (Holton 1967), and their combination (Du and Rotunno 2014). They have a wind maximum within the planetary boundary layer (PBL) and their intensity and direction often follow a clear diurnal cycle, peaking overnight (Blackadar 1957; Holton 1967; Bonner 1968; Shapiro et al. 2016). A second type is synoptically related LLJs, termed by some as low-level jet streams (LLJSs; Stensrud 1996), which result from tight pressure gradients in synoptic systems and are often linked to upper-level jet streaks via ageostrophic transverse circulations. These LLJs tend to be more elevated, have a larger vertical extent compared to NLLJs, and often lack clear diurnal cycles (Hoecker 1963; Uccellini 1980; Chen et al. 1994; Du et al. 2012, 2014). Characteristics of both types of LLJs have been documented in the context of the SALLJ (Salio et al. 2002; Nicolini et al. 2004a; Rife et al. 2010; Repinaldo et al. 2015; Oliveira et al. 2018), but the specific mechanisms are still not well understood owing in part to a lack of routine high spatially and temporally resolved ground and upper-air observations in the path of the jet.

The first extensive observations of the SALLJ came from the South American Low-Level Jet Experiment (SALLJEX; Vera et al. 2006), which included a special observing period with observations from an upper-air network and aircraft from early January to mid-February 2003. The project was centered in Bolivia where the peak winds of the SALLJ are thought to occur (Byerle and Paegle 2002; Salio et al. 2002; Campetella and Vera 2002; Silvers and Schubert 2012). These observations documented an overnight peak in SALLJ intensity; however, despite improvements in temporal resolution (soundings up to four times daily) the exact timing of the peak SALLJ winds could not be resolved. A summertime low-level wind gyre was also found within the SALLJEX study region with a clearer wind rotation when a LLJ was present. These SALLJEX findings linked the jet timing to a combination of an inertial oscillation, a subsynoptic pressure

gradient related to mountain–valley differential diurnal heating, and a dominant meridional mean wind (Nicolini et al. 2004a; Vera et al. 2006). While prior research stemming from SALLJEX observations has emphasized small-scale processes that produce mean SALLJ profiles with wind speed peaking below 850 hPa, jets cores as high as 3 km AGL were also noted.

Besides SALLJEX, most of our knowledge of the SALLJ in central Argentina comes from reanalysis, modeling, and satellite studies. Multiple reanalysis studies also found that the majority of SALLJs in this region do peak below 1500 m or about 850 hPa (Salio et al. 2002; Rife et al. 2010; Oliveira et al. 2018; Montini et al. 2019). However, Oliveira et al. (2018, hereafter ONK18) found a significant number of more elevated jets. They determined that strong site-to-site variability in SALLJ heights across subtropical South America motivated the need for localized LLJ identification methods. ONK18 created more flexible criteria than was previously applied (Bonner 1968; Nicolini and Saulo 2000; Salio et al. 2002) by searching height ranges rather than specific pressure levels (e.g., 850 and 700 hPa in Nicolini and Saulo 2000), deepening the layer for LLJ identification, and removing a weak zonal component requirement. These criteria allowed more days with SALLJs to be identified throughout South America than previous studies (ONK18's Figs. 3 and 6), including more instances of elevated SALLJs with strong zonal components. They hypothesized that the propensity for elevated LLJs was related to synoptic-scale baroclinic systems, but emphasized the need for additional studies on the patterns and forcing mechanisms controlling the elevated LLJs in southeastern South America.

Modeling studies have emphasized synoptic environments that might contribute to the presence of the SALLJ in central Argentina. The subset of jets that extend past 25°S have been linked to the deepening of the thermo-orographic northwest Argentina low (NAL), which may help to lengthen the meridional flow and extend the jet south into Argentina (Nicolini and Saulo 2000; Salio et al. 2002; Nicolini et al. 2004b). The NAL is a semipermanent feature during the summer due to strong surface warming, but orographic subsidence linked to transient activity modulates its intensity (Seluchi et al. 2003). Strong lee cyclogenesis occurs ahead of upper-level troughs traversing the Andes in connection with the occurrence of MCSs (Rasmussen and Houze 2016) and could be partially responsible for strengthening the NAL and therefore enhancing the SALLJ. Unlike NLLJs driven by boundary layer processes, this intensification of the gradient due to lee cyclogenesis does not depend on the diurnal cycle and could be responsible for the extension of the SALLJ above the PBL (Uccellini 1980; Saulo et al. 2004). Additionally, the importance of the South Atlantic subtropical high, located to the east of the SALLJ, in strengthening the pressure gradient associated with the SALLJ is not well understood. Salio et al. (2002) found that these SALLJs lasted 1–10 days with those with longer durations being less frequent. Past work has provided hypotheses for drivers of the SALLJ from boundary layer processes to synoptic gradients, but limited observations have failed to deduce the relative importance of these processes to various instances of the SALLJ. Increased observations of the SALLJ will help to connect characteristics of the SALLJ to the various hypothesized mechanisms and provide new insights into the nature of the phenomena.

The Remote sensing of Electrification, Lightning, And Mesoscale/microscale Processes with Adaptive Ground Observations (RELAMPAGO; Nesbitt et al. 2021) field campaign took place in late 2018 in central Argentina, deploying a broad array of instrumentation including soundings in the path of the SALLJ up to every 3 h around forecasted convectively active periods. The main period of the campaign was from 1 November to 17 December 2018 and focused farther south than SALLJEX. Prior to RELAMPAGO, no routine soundings were available east of the Andes foothills in central Argentina with enough temporal resolution to capture the variability of the SALLJ that feeds directly into the developing convection. The study region of RELAMPAGO in central Argentina lies in an area that is a maximum in days with a LLJ present (Nicolini and Saulo 2000; Oliveira et al. 2018), often near the terminus of the SALLJ (Paegle 1998; Salio et al. 2002), and where the SALLJ occurs within the vicinity of the Sierras de Córdoba (SDC; see Fig. 1), a mesoscale mountain range east of the Andes and a focal point for convective initiation and rapid upscale growth to MCSs (Romatschke and Houze 2010; Rasmussen and Houze 2011, 2016; Rasmussen et al. 2014; Mulholland et al. 2018). It has been hypothesized that the modification of the SALLJ by the SDC could partially explain the frequent convective initiation and upscale growth into MCSs in this region (Rasmussen and Houze 2016).

This study presents an observational analysis of the SALLJ during the RELAMPAGO campaign using frequent soundings from two fixed stations in the path of the jet, providing an unprecedented look at characterizing (e.g., timing, peak speed, direction, height) the SALLJ near the SDC. Reanalysis data are then used to fill in the spatial and temporal observational gaps and to expand on the thermodynamic influences of the SALLJ. This detailed analysis of the SALLJ during varying synoptic-scale environments allows for links between environments on many scales and characteristics of the SALLJ. To our knowledge, this study presents the first look at the SALLJ near the SDC using high temporal observational data. Additionally, recently released reanalysis data has higher temporal and spatial resolution than past reanalysis data used for LLJ studies in this region. The objectives of this study are to 1) develop objective criteria for identifying the SALLJ near the SDC, 2) describe the variability in the vertical and temporal structure of the SALLJ observed during RELAMPAGO, 3) link variability in jet height and duration to synoptic and subsynoptic processes, and 4) investigate moisture transport and the presence of convection during periods of SALLJ activity.

2. Data and methods

a. *Fixed soundings*

Throughout the RELAMPAGO period (1 November–17 December 2018), soundings were launched at two fixed sites positioned in the path of the jet (Fig. 1): Córdoba (COR;

TABLE 1. Number of soundings with LLJs identified (percentage of total launched) at COR and VMRS for both the Oliveira et al. (2018) criteria and our modified criteria.

		No. of LLJs identified		
	Total soundings	Oliveira et al. (2018) criteria	Modified criteria	Percentage increase in LLJ
COR	175	60 (34.3%)	67 (38.3%)	11.7%
VMRS	136	81 (59.6%)	89 (65.4%)	9.9%

31.298°S, 64.212°W; elevation: 490 m) and Villa de María del Río Seco (VMRS; 29.906°S, 63.726°W; elevation: 341 m). The operational COR site lies just to the east of the SDC, and the sounding frequency was increased for RELAMPAGO to characterize the near-convective environment. The VMRS site is farther north and is unique to RELAMPAGO. VMRS was selected specifically to monitor the SALLJ airmass characteristics before it was ingested by convective storms forming to the south and therefore sounding launches were heavily weighted toward periods of expected SALLJ activity. The default launch frequency during the campaign was two times per day (0000 and 1200 UTC) at COR and once a day (0900 UTC) at VMRS. Soundings were launched every 3 h (i.e., eight per day) during intense observation periods (IOPs), with two short periods of hourly soundings at COR and one at VMRS. A total of 175 and 136 soundings were launched at COR and VMRS, respectively (Table 1). About three-quarters of the soundings at both stations were launched during the IOPs, but there is a clear bias toward default launch times: around half of the soundings at COR and a third at VMRS. The winds from these soundings were used to identify LLJs and their characteristics (e.g., timing, peak speed, direction, height). The sounding sites were operated by the Servicio Meteorológico Nacional (SMN) and all radiosondes used were Modem GPSonde M10 with 2-s vertical resolution (Servicio Meteorológico Nacional—Argentina 2019).

Two types of automated data quality checks (gross limit and rate of change checks) and a manual visual examination were carried out by NCAR/EOL Processing and Quality Control (UCAR/NCAR–Earth Observing Laboratory 2020). Additionally, low-level winds in LLJ soundings were examined for convection contamination. A qualitative inspection was conducted using saturated layers in the soundings and *GOES-16* IR brightness temperatures to determine the presence of convection. Using this method, about one-fifth of the soundings had clouds present, but only a handful were identified as sampling convection. Convection did not appear to affect the low-level winds in any of the soundings, but three soundings within deep convection extending from the low levels on 12 November at VMRS were not included in the statistics out of caution.

b. Identification of LLJs

The criteria used in this study to identify the SALLJ during the RELAMPAGO campaign are based on ONK18's method. A LLJ was identified by ONK18 when 1) winds displayed a local maximum in speed within the lowest 3000 m AGL and the maximum was equal or greater than 12 m s^{-1}, and 2) the wind speed decreased by at least 6 m s^{-1} from the maximum speed to the first minimum found aloft or to the speed at 4000 m AGL, whichever occurred first. While the ONK18 criteria captured elevated jets better than past criteria, it did not identify LLJs during widespread convective events during RELAMPAGO when the jet was broader and elevated. For example, the ONK18 criteria failed to identify a LLJ in the 1200 UTC 12 November and 0900 UTC 13 December observational soundings at COR (Fig. 2) due to the deep layer of strong winds. Therefore, modifications were made to the ONK18 criteria to capture vertically broader and more elevated LLJs observed in the RELAMPAGO sounding dataset by deepening the layers over which to search for the wind minimum aloft

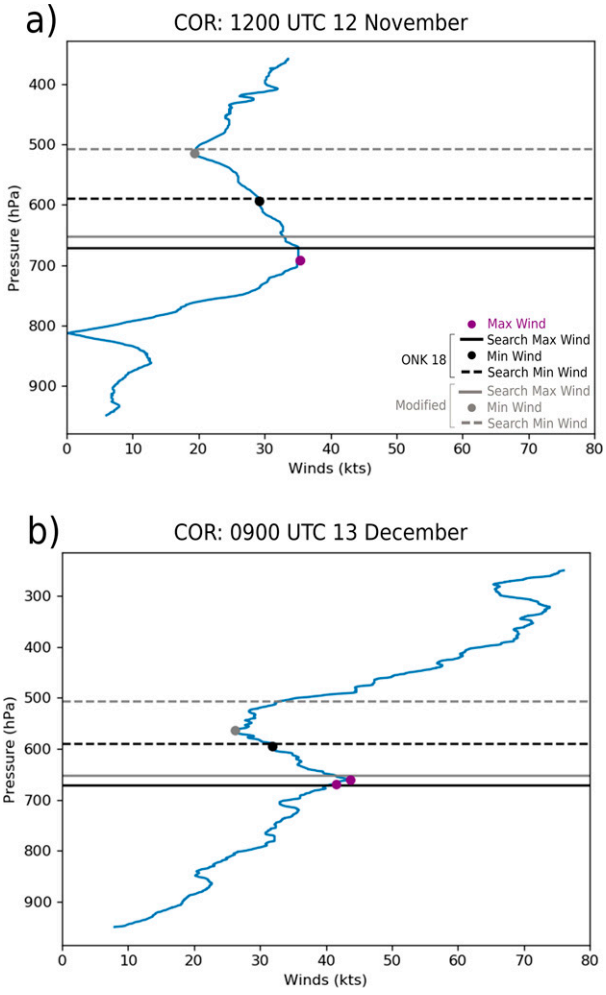

FIG. 2. Example vertical wind profiles from COR soundings showing application of the LLJ identification criteria: (a) 1200 UTC 12 Nov and (b) 0900 UTC 13 Dec 2018. Wind speed maximum (purple dot), minimum (black dot) found by Oliveira et al. (2018) criteria and minimum found by the modified criteria used in this study (gray dot) are indicated in each figure. The lines mark the top of the search areas for wind maxima (solid) and minima (dashed lines) for the two criteria.

and for the wind maximum, respectively. A RELAMPAGO wind profile therefore must meet the following two criteria to be identified as a LLJ:

- Winds must display a local maximum in speed within the lowest 3200 m AGL and the maximum must be equal to or greater than 12 m s^{-1} (23.33 kt).
- The wind speed must decrease by at least 6 m s^{-1} (11.66 kt) from the maximum speed to the first minimum found aloft or to the speed at 5700 m AGL, whichever occurs first.

The height thresholds were modified to identify the profiles with clear maximums in wind, breaking from the broad background trend of increasing wind with height, while minimizing changes from the ONK18 criteria. By allowing the minimum to be found higher, we capture the minimum in both soundings shown in Fig. 2. Additionally, the combination of the two modifications captures the maximum and minimum for the 0900 UTC 13 December sounding and allows it to be classified as a LLJ. The hierarchy established in ONK18 for dual-core or wide-core LLJs has been preserved with the strongest and lowest jet core classified as the LLJ in these scenarios. Dual-cored LLJs were not commonly observed during RELAMPAGO (less than 10% of LLJs) and given the limited sample size, a more detailed analysis on their potential impact was not conducted. The modified criteria better identify persistent and elevated jets that bring significant moistening to the lower levels and are associated with times of widespread convection in this region, as will be shown in the results section below. Note Fig. 2 shows how the criteria, based upon height, align with pressure coordinates that will be used throughout the analysis.

c. *European Centre for Medium-Range Weather Forecasts Re-Analysis (ERA5)*

ERA5 is the fifth generation of atmospheric reanalysis produced by the European Centre for Medium-Range Weather Forecasts (ECMWF; Hersbach et al. 2020). It has hourly output and a horizontal resolution of 31 km on 37 pressure levels. The vertical resolution is 25 hPa from 1000 to 750 hPa and 50 hPa from 750 to 450 hPa. Compared to past reanalysis datasets that covered this region (e.g., Climate Forecast System Reanalysis, NCEP–NCAR reanalysis, ERA-Interim), ERA5 has increased temporal, spatial and vertical resolution. ERA5 hourly winds, heights, and specific humidity are used in this study to supplement the fixed soundings launched during RELAMPAGO and put the observations in a broader spatial and temporal context. From our investigation (appendix A), the evolution of synoptic-scale ERA5 wind and moisture patterns are adequate for addressing this study's objectives. While only about half of the observed LLJs were identified when applying our modified criteria to the ERA5 data, periods of enhanced northerly winds and increased moisture match those observed by the soundings and are considered a sufficient proxy for LLJ events for our study. The ERA5 analysis in this study is conducted within the following domains: South America (5°N–55°S, 35°–95°W) for the synoptic maps, and the geographical domain of the SALLJ (10°–50°S, 55°–65°W) for the Hovmöller diagrams.

d. *Geostationary Operational Environmental Satellite R-Series (GOES-R)*

GOES-16 IR brightness temperatures with a horizontal resolution of 2 km and temporal resolution of 15 min were used to determine spatial coverage of convection throughout the campaign. A brightness temperature threshold of 235 K was used within the box defined by 29°–35°S, 55°–66°W (black box Fig. 1b). This area covers the intersection of the SDC and the terminus of the SALLJ. The threshold of 235 K was used for detecting clouds associated with convection in different regions of South America, as in Vila et al. (2008) and Carvalho and Jones (2001).

3. Results

a. *Variability in the SALLJ*

The number of LLJs found during RELAMPAGO using the ONK18 criteria and our modified criteria is shown in Table 1. A higher percentage of soundings at VMRS were identified as LLJs than at COR. The lower frequency of LLJs at COR could be explained by blocking of the LLJ by the SDC, which would not occur farther north at VMRS. However, the timing of when soundings were launched (i.e., preferential launches at VMRS during forecasted SALLJ periods) likely biased the result as well. The modified criteria resulted in about 4%–6% more soundings containing LLJs than using ONK18 (a 10%–12% increase in LLJs), but more important to this analysis are the times when these additional LLJs were identified. Time series of the v-component of the wind from soundings launched during RELAMPAGO at COR and VMRS are shown in Figs. 3 and 4, respectively, where red indicates northerly flow and blue southerly. The height of maximum wind (jet core) is indicated for soundings with LLJs defined by the ONK18 criteria (black squares) and those added when using the more relaxed modified criteria described in the Methods section (gray × symbols). During RELAMPAGO, northerly flow varied in duration and depth. The majority of periods of strong northerly winds lasted for around 2 days or less; however, there were three longer-duration periods (~3–6 days): 8–12 November, 19–22 November, and 8–13 December (black boxes in Figs. 3 and 4). Overall, the jet core winds were generally below 750 hPa, but more elevated and vertically broader northerly LLJs were captured using the modified criteria (~700 hPa; gray circles), primarily near the end of the longer-duration periods. Widespread convective events near the SDC were also observed near the end of these same longer-duration jet periods (e.g., Piersante et al. 2021). The modified criteria will therefore hereafter be used to characterize the SALLJ in this study.

Figures 5–7 provide objective quantifications of the variations in direction, speed, height, and timing of the SALLJ sampled during RELAMPAGO. Figure 5 shows that the majority of LLJs were found to be from a northerly direction (between NW and NE) at both stations. Jets from the NNW

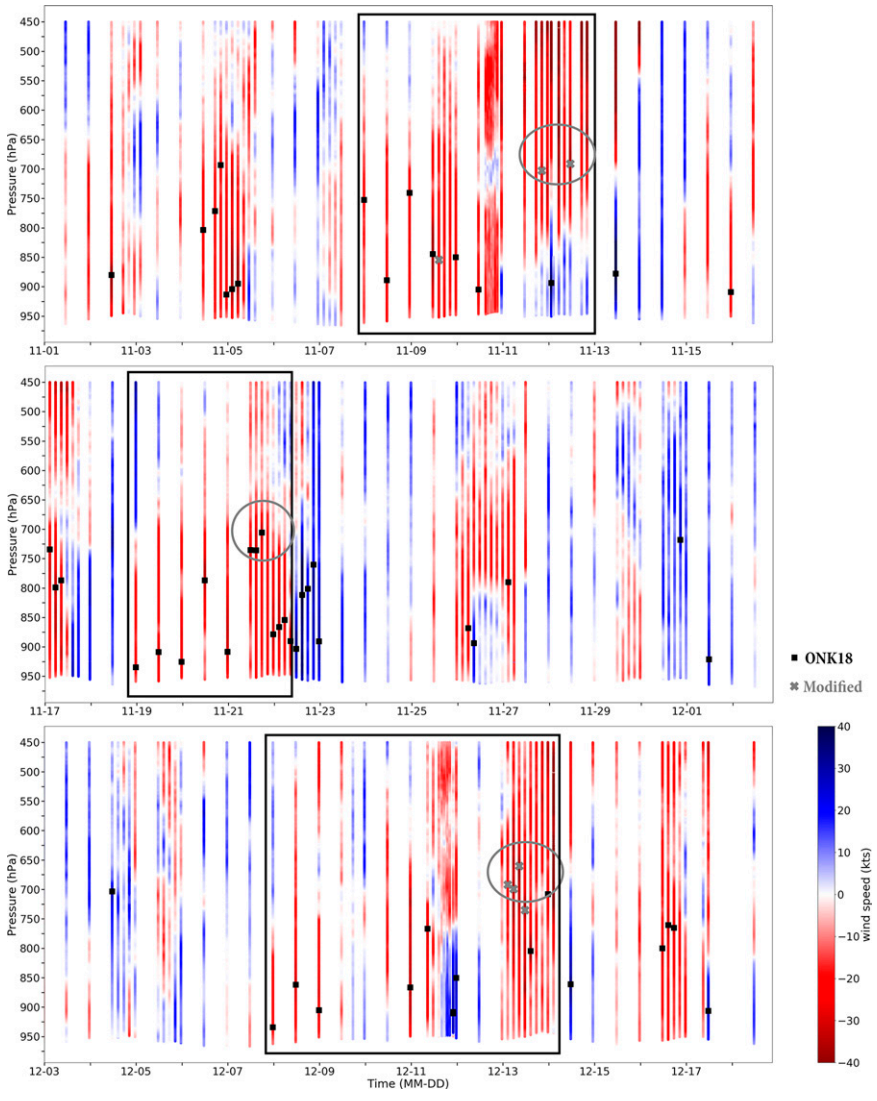

FIG. 3. Time series of the v component of the wind from soundings launched during the RELAMPAGO campaign at COR, with red indicating the v component is from the north and blue from the south. The level of maximum wind (jet core) is shown for soundings with an LLJ identified from Oliveira et al. (2018) criteria (black squares) and additional LLJs found when applying our modified criteria (gray × symbols). The black boxes highlight the three longer-duration periods of northerly flow and the gray circles highlight elevated/vertically broader LLJs near the end of the events.

were more common at VMRS than COR and the percentage from the NNW at COR is even further reduced when the elevated and vertically broader LLJs found by the modified criteria are removed (not shown). Terrain north and west of COR reaching heights between 1000 and 2000 m, as part of the SDC (Fig. 1c), likely blocks low-level winds below ~850 hPa and is responsible for the lower frequency of NNW jets at COR compared to VMRS.

Stronger LLJs were observed more often at VMRS than COR (Figs. 5 and 6a,d). The distribution of maximum wind speeds is skewed toward weaker winds at COR with a median of ~29 kt, while at VMRS the distribution was more uniform and had a median of ~32 kt. A comparison of LLJ core wind speeds when the jet was observed at both stations at the same time verified that VMRS often tended to have higher max wind speeds than COR. This agrees with past modeling work that found wind speeds increased northward to a peak in Bolivia/Paraguay (Byerle and Paegle 2002; Salio et al. 2002; Campetella and Vera 2002; Silvers and Schubert 2012). However, the jet core winds associated with elevated and broader LLJs tended to be more similar in intensity at the two stations (not shown).

In terms of the level of maximum wind, both stations have a greater frequency of LLJs in the lower levels, particularly at

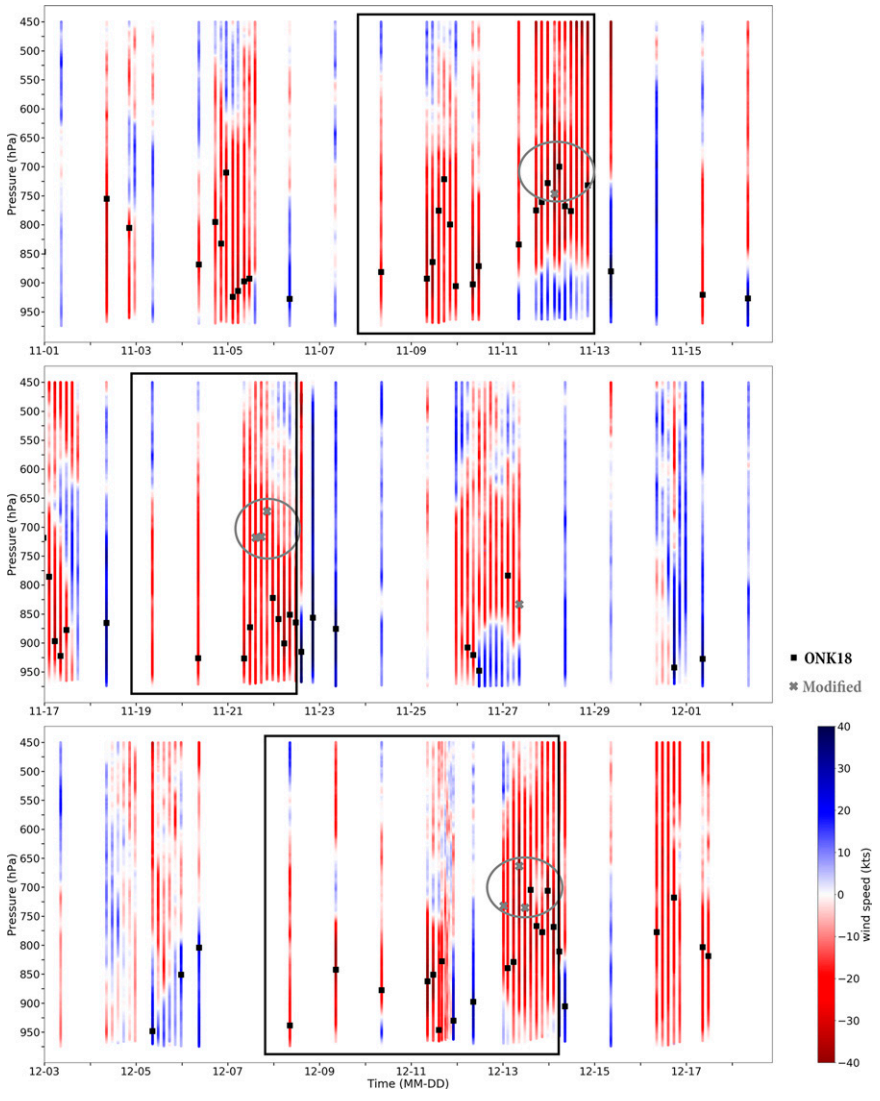

FIG. 4. As in Fig. 3, but for VMRS.

COR (Figs. 6b,c,e,f). At both stations, about half of the LLJs peaked in the lowest 100 hPa (from 950 to 850 hPa; ~1000 m AGL) with the other half peaking above 850 hPa. Notably, jet cores were found up to 650 hPa. With a once daily 15-yr dataset, ONK18 found that about 20%–25% of jets in southeastern South America and 39% of northerly jets at COR displayed a core above 1500 m AGL. Similarly, this study, using a more diurnally complete dataset, found 38% and 39% of all jets at COR and VMRS, respectively, had cores above 1500 m AGL (Figs. 6c,f), although this result is limited to one spring/early summer season.

For the remainder of this study, we will focus on northerly LLJs because their transport of moisture likely contributes to organized convection in this region, as will be discussed later, and next explore the temporal variability of these northerly LLJs. A key difference between NLLJs and LLJSs is the presence of a diurnal cycle (e.g., Stensrud 1996), with NLLJs more frequent and intense overnight. To investigate a potential diurnal cycle and reduce launch bias, we only consider 24-h periods with at least seven 3-hourly soundings available, which constituted about a fifth of the 45-day campaign. Figure 7 shows that the highest percentage of LLJ soundings occurred overnight into the early morning (between 0300 and 1200 UTC) with the lowest percentage during the afternoon (1500–1800 UTC). The finding of a nocturnal peak in LLJ identification is consistent with past studies describing NLLJs in South America (Salio et al. 2002; Nicolini et al. 2004a; Marengo et al. 2004).

From the observational soundings (Figs. 3 and 4), SALLJ periods of varying duration were identified. ERA5 is used to fill in potential observational gaps in the duration of northerly flow periods, which serve as a proxy for LLJ activity that will later be linked to synoptic-scale processes. Figure 8 is a north–south Hovmöller diagram of ERA5 850-hPa v wind

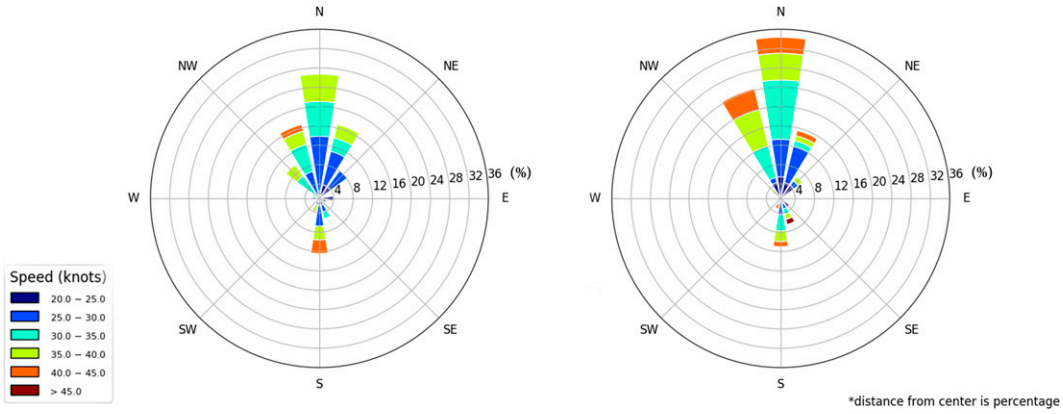

FIG. 5. Wind roses showing the percentage of all LLJ soundings with a specific wind direction and wind speed (color shading) at jet core height using the modified criteria at (left) COR and (right) VMRS.

where the *y* axis is latitude, showing the spatial and temporal extent of enhanced periods of northerly flow at various latitudes. The ERA5 hourly data contain periods of persistent 850-hPa northerly low-level flow at COR and VMRS. Five of these periods last for around 2 days or less (solid gray circles) and three periods last for longer than 2 days (black boxes), matching those highlighted from observations (Figs. 3 and 4).

The 19–22 November SALLJ period is distinct from the 8–12 November and 8–13 December periods in several ways: 1) northerly flow is present for 3–4 days rather than 5–6 days, 2) the period does not end with a persistent elevated jet and rather becomes less elevated before the flow switches to southerly (Figs. 3 and 4), and 3) the northerly flow at the beginning of the 19–22 November period is weak at 850 hPa (dashed black box in Fig. 8) as the wind maximum is very shallow (Figs. 3 and 4). Due to the extended duration of northerly flow and a persistent, elevated jet at the end of each period, 8–12 November and 8–13 December will be defined as 5–6-day SALLJ events and the shorter periods (including 19–22 November) are defined as shorter-duration events. Note that the SALLJ events are defined by persistent 850-hPa northerly flow in ERA5 and thus a jet is not necessarily occurring constantly throughout that event. While the two 5–6-day events are of similar length and both feature persistent northerly flow, they have quite different flow patterns. From 8 to 12 November, the magnitude of northerly flow was relatively consistent, while during the 8–13 December event, the northerly flow varied in magnitude with three closely spaced bursts of stronger northerly wind (Fig. 8).

Overall, RELAMPAGO observations largely confirmed characteristics of the SALLJ in central Argentina inferred from previous reanalysis and modeling studies in that the majority of the SALLJs are from the north, peak in the lower levels overnight, and are present for 2 days or less. However, there are SALLJ events of longer duration with observed elevated LLJs near the end of each of the events that warrant closer study in linking jet characteristics to the conditions under which they form.

b. *SALLJ characteristics*

To explore the evolution of the SALLJ in more detail, the v-wind component was plotted from soundings at COR on days when more than six 3-hourly soundings were available and a LLJ was identified (Fig. 9). COR is shown because more soundings are available, but similar conclusions can be drawn at VMRS and any important differences will be highlighted. These SALLJ days were then split into two categories based upon the level of maximum wind. Those SALLJs that peaked below 825 hPa were classified as boundary layer LLJs and those above 825 hPa as elevated LLJs. The 825-hPa level was chosen as it is the approximate delineation between jet core groupings found from all RELAMPAGO SALLJ observations (Figs. 6b,d).

Using the above requirement for sounding frequency, four boundary layer LLJ days (5, 17, 22, and 26 November) were identified during RELAMPAGO. These boundary layer LLJs occurred during the shorter-duration events (Figs. 3, 4 and 8). The general characteristics are similar across all of these boundary layer LLJ days and are represented here by soundings from 5 and 22 November (Figs. 9a,b). The boundary layer jet-period characteristics are as follows: 1) jet core below 825 hPa (by definition), 2) v component of the jet strongest overnight/early morning (red circle), and 3) a switch to southerly low-level winds after the northerly SALLJ weakens (blue circle). At VMRS the boundary layer LLJs displayed similar characteristics, but the switch to southerly low-level winds was shifted a couple hours later and southerly winds were weaker in the afternoon. Most of the characteristics of these boundary layer type LLJs resemble those of NLLJs; however, the switch in the low-level wind to southerly appears to be related to synoptic-scale forcing and possible frontal passages. The delay in this switch to the south between COR and VMRS is consistent with frontal boundaries progressing northward with time and will be discussed in a later section.

Two elevated LLJ days were identified using the above requirement for sounding frequency, occurring near the end of 8–12 November and 8–13 December SALLJ events. These elevated jets did not exhibit the characteristics associated with

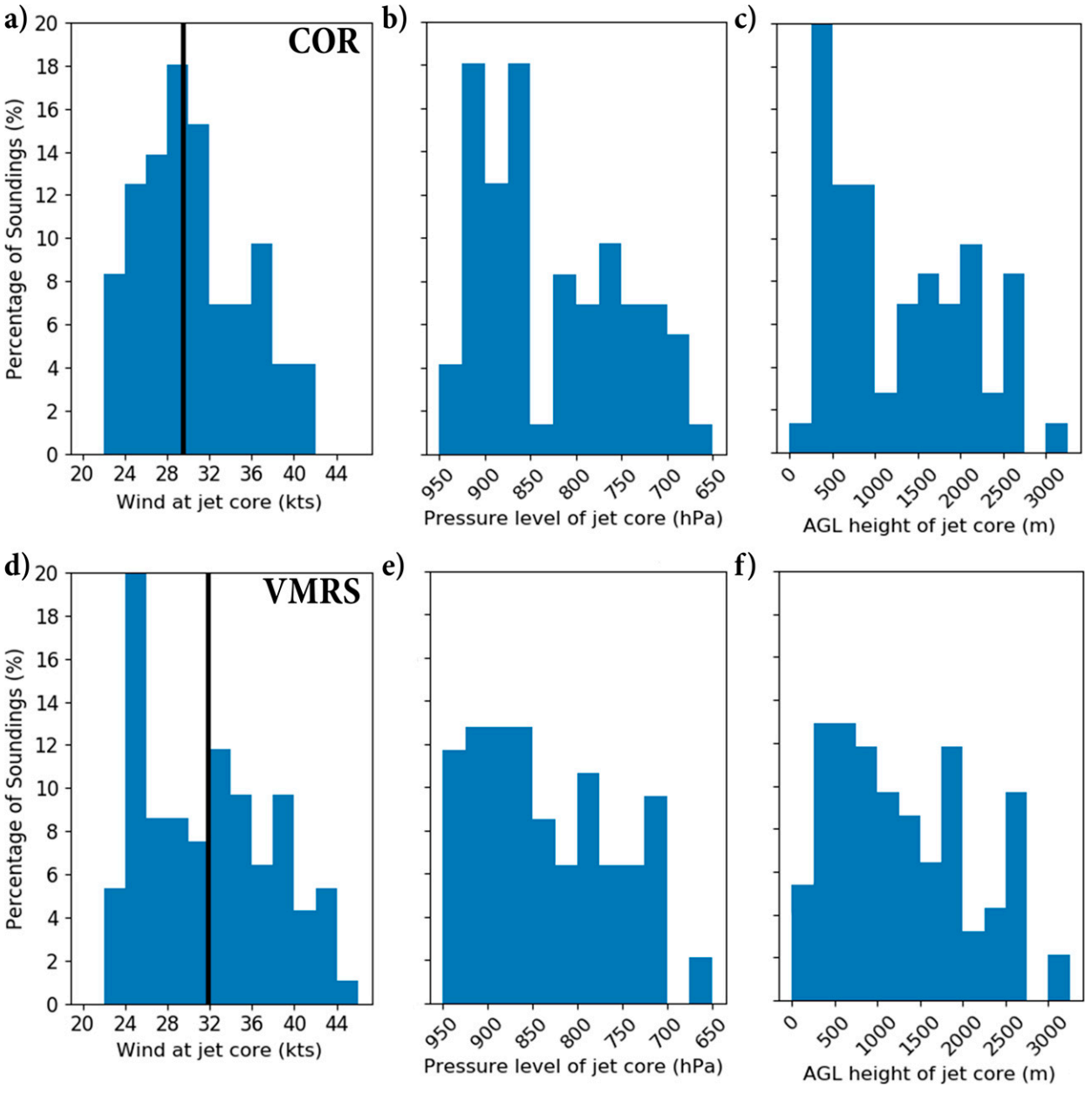

FIG. 6. Histograms of LLJ core wind speeds and the pressure levels/above ground level heights at which they occurred for (a)–(c) COR and (d)–(f) VMRS. The black lines are median jet core wind speeds.

the boundary layer LLJ days and have important differences from one another (Figs. 9b,c). Two general observations can be made of these elevated LLJs: 1) the jet core was more elevated than the boundary layer days (by definition); between 825 and 550 hPa and 2) there was not a clear diurnal trend in peak SALLJ intensity.

For the 12 November soundings (Fig. 9c), the wind profiles were similar throughout the day. Winds above 800 hPa were continuously from the north; however, a LLJ was identified only once on this day (1200 UTC; Figs. 3 and 9c). In many profiles when the peak northerly winds are elevated, there is not a clear decrease in wind above the maximum, and this lack of a distinct jet core meant many soundings during this day did not meet the LLJ criteria. Calm to southerly wind was also present in the lower levels during this period, possibly connected to the southerly flow associated with the western side of a lee cyclone and the associated frontal passage (Piersante et al. 2021). At VMRS, the jet was slightly less elevated with distinct jet cores resulting in more LLJs identified than at COR (not shown). Unlike 12 November, the wind profiles on 13 December (Fig. 9d) fluctuated in intensity and no discernable temporal pattern in jet core height or intensity

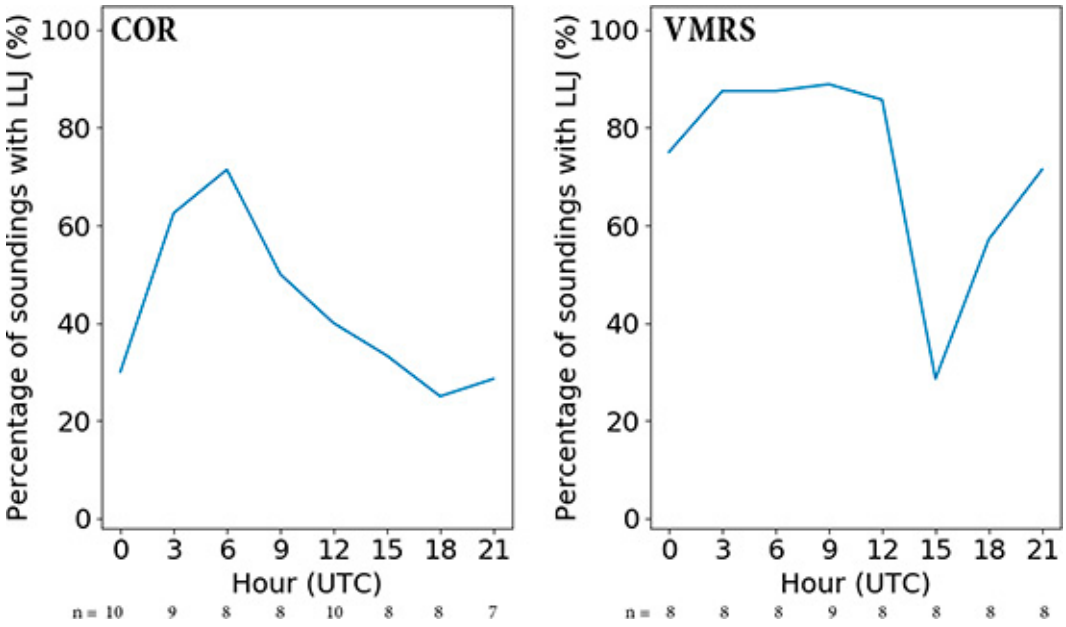

FIG. 7. Percentage of soundings at each hour with northerly LLJs identified for (left) COR and (right) VMRS. Note that local time is UTC − 3 h. The number of soundings analyzed at each time is shown below the hours.

was found. The LLJ was present in separate pulses in the lower levels during this event before being more elevated on 13 December (Figs. 3 and 4). Overall, the distinct temporal and vertical characteristics between the boundary layer and elevated LLJs imply different mechanisms might be important for jet formation and evolution that may vary on a case-by-case basis.

To investigate the possibility of boundary layer processes affecting the SALLJ, the wind direction in the low levels (900 hPa, similar to Nicolini et al. 2004a) was plotted for all 4 boundary layer jet days (Fig. 10a) separately from the two elevated days (Fig. 10b). A clear rotation of low-level wind directions can be seen during the boundary layer days: northeasterlies occurred overnight (0000–0600 UTC), northwesterlies in the morning (0600–1500 UTC) and a switch to southerlies in the afternoon (0900–2100 UTC). The backing of the winds with a northerly component in a 24-h period for the boundary layer days is consistent with a role of diurnal processes such as the inertial oscillation affecting the winds (Blackadar 1957). However, each boundary layer day differs in the timing of the switch to southerlies. This switch occurred as early as 0900 UTC on one day and as late as 1500 UTC on another day, indicating that synoptic drivers (e.g., upper-level troughs and associated frontal boundaries) may also play a role in the timing of the boundary layer jets, particularly the switch to southerly winds.

In contrast to the boundary layer days, no sustained diurnal progression in low-level wind direction was observed during the elevated days. It appears that the elevated days are largely synoptically driven and the synoptic winds overwhelm potential diurnal cycles from boundary layer processes. Additionally, as these elevated days occurred at the end of the longest duration 5–6-day SALLJ events, widespread clouds from prolonged moisture transport by the jet may have dampened diurnal cycles due to the lack of heating. Similar to the boundary layer jet days was a switch to deep southerly wind that ended the northerly elevated LLJs and the overall shorter and 5–6-day SALLJ events (Figs. 3 and 4). This switch in the winds is likely a result of southerly flow on the western edge of the lee cyclone associated with the westward progression of the upper-level pattern and the associated passage of a surface-based front (Piersante et al. 2021). Frontal passages were stronger, reinforced by strong synoptic forcing, in the 5–6-day SALLJ events and are therefore easier to identify with the limited observations available in this region than those during shorter-duration events (SMN analyses: http://catalog.eol.ucar.edu/relampago/surface).

c. *Large-scale forcing*

In this section, we explore the hypothesized relationship of the SALLJ peak timing, height, and duration to the presence and timing of upper-level disturbances and associated low-level responses. All SALLJ events during RELAMPAGO (gray circles and black boxes in Fig. 8) coincided with a 500-hPa trough over the Pacific Ocean and an 850-hPa trough in the lee of the Andes. In each event, the upper-level trough passage over the Andes resulted in low-level lee cyclogenesis broadly controlling the low-level northerly flow in the SDC region, despite variations in latitude and amplitude of these troughs during each SALLJ event. The progression speed of the upper-level pattern also varied between events, which had an impact on the duration of northerly flow.

To look further into this relationship between the progression of the upper-level pattern and the timing and duration of

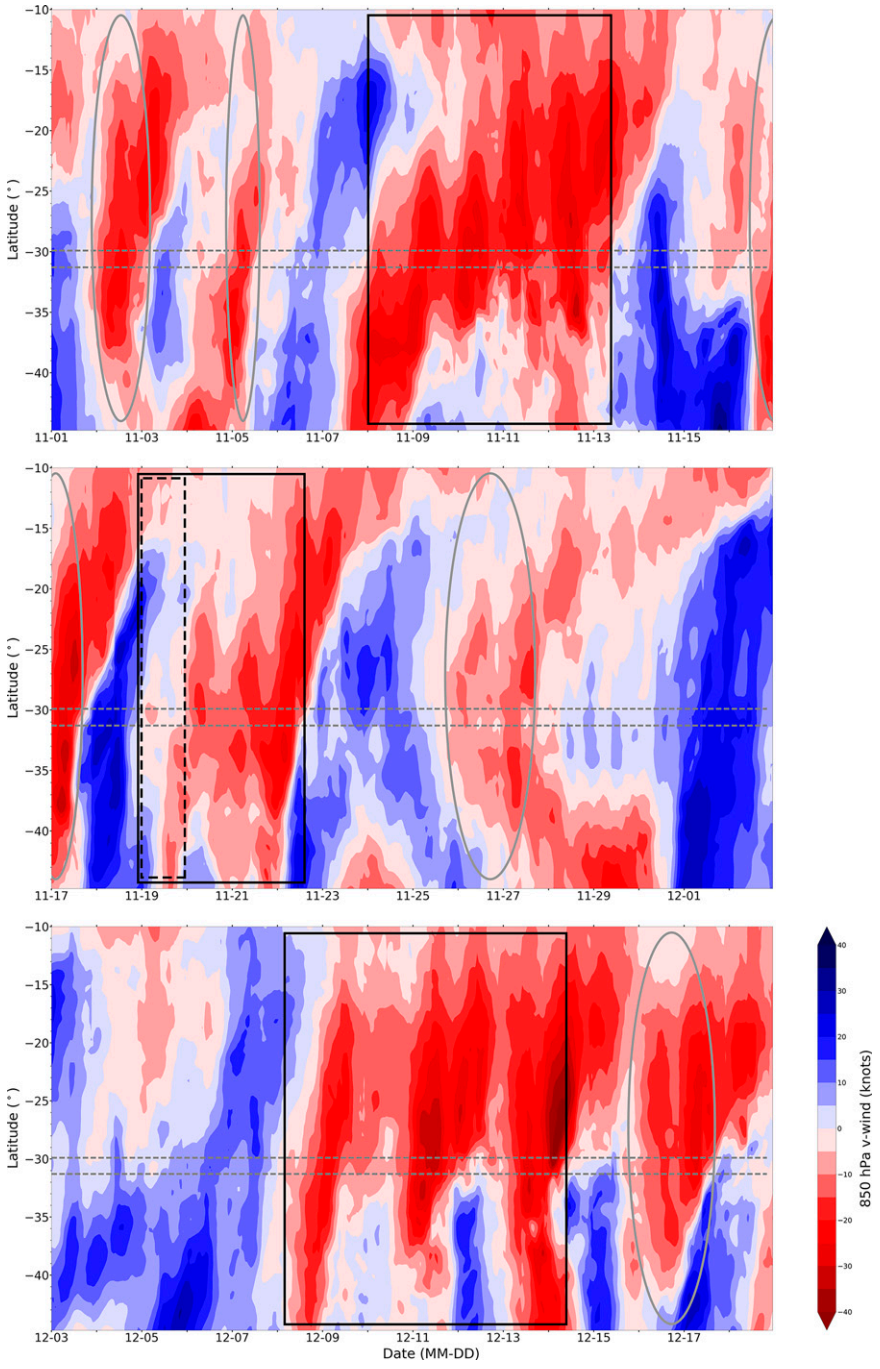

FIG. 8. North–south Hovmöller diagram of the v component of the wind at 850 hPa averaged over 55°–65°W using ECMWF Re-Analysis 5 (ERA5). Red is wind from the north and blue is wind from the south. Dash–dotted lines show the latitude of VMRS (northern) and COR (southern). Instances where a northerly SALLJ is seen in central Argentina are highlighted with black boxes (5–6-day SALLJ events) and gray circles (shorter SALLJ events). The dashed black box highlights the weaker flow at 850 hPa at the beginning the 19–22 Nov event.

low-level northerly flow, the 500- and 850-hPa heights and 850-hPa winds are shown in 12-h increments for the 19–22 November event (Fig. 11). During this event, an upper-level shortwave at 500 hPa (red circles) approached the southern Andes by 1200 UTC 21 November (Fig. 11d). As this shortwave impinged on the Andes, the response was an 850-hPa lee trough (orange boxes) over the sounding sites (red dots). The shortwave was south of the region where the 850-hPa lee

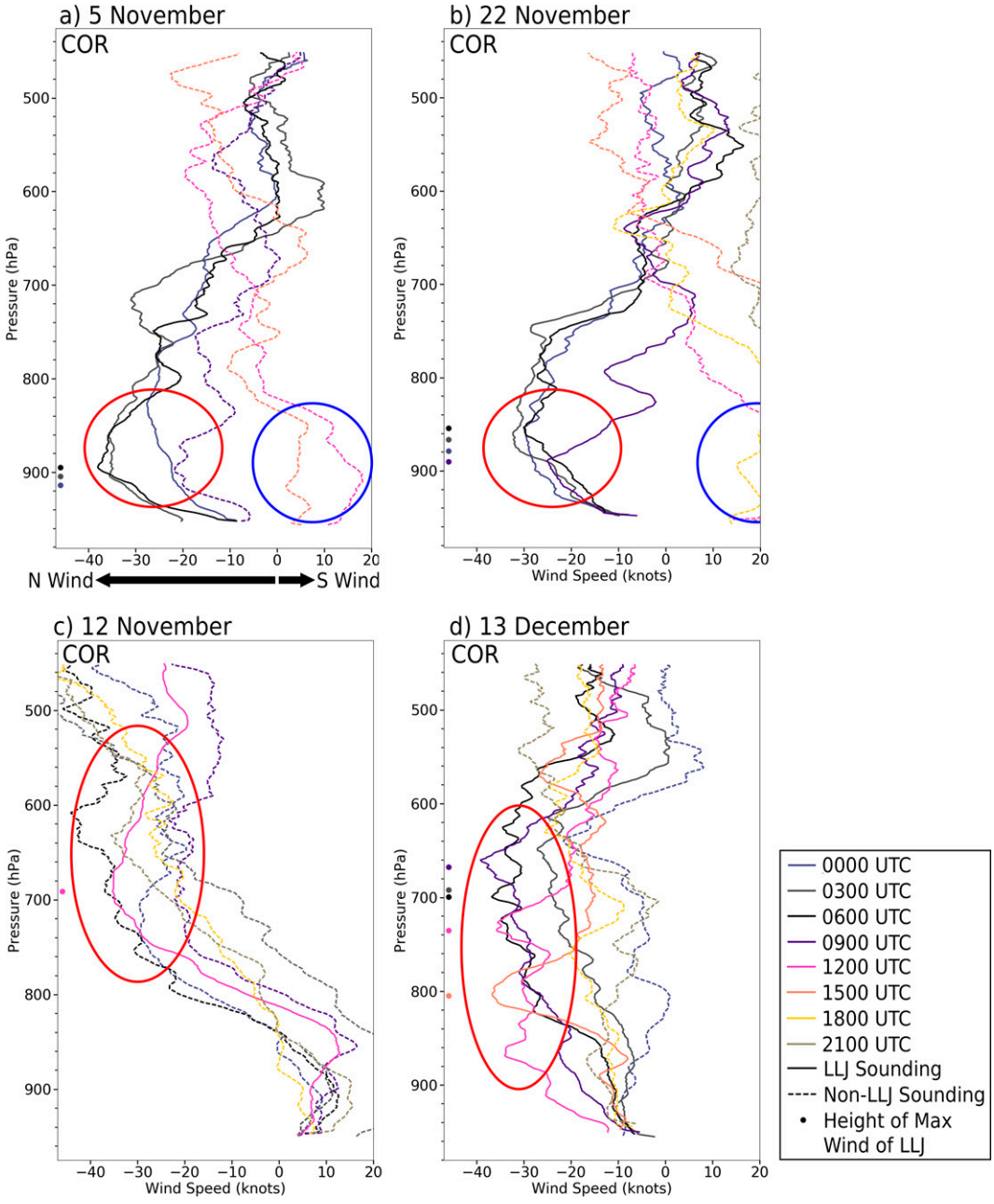

FIG. 9. The v component of the wind for soundings from 24-h periods at COR from (a) 5 Nov, (b) 22 Nov, (c) 12 Nov, and (d) 13 Dec 2018. The time of the sounding is indicated by color, the solid lines indicate soundings meeting the LLJ criteria using the full wind, and the dots show the pressure level of the jet core. The range of heights of the strongest winds from the north (south) is highlighted in the red (blue) circles.

troughing formed and where the SALLJ strengthened; therefore, it is likely that the 850-hPa high pressure to the east (blue circle) also contributed to the strengthening of the SALLJ. As the upper-level shortwave came ashore, the lee troughing strengthened, as seen by the north and then eastward movement of the lowest 850-hPa heights (and the edge of northerly flow; Fig. 8) between 0000 and 1200 UTC (Figs. 11e,f). Peak low-level northerly flow extended southward to about 40°S at 0000 UTC 22 November (Fig. 11e). By 1200 UTC that same day, lee cyclogenesis occurred slightly northwest of SDC region, causing northerly flow to recede up to 30°S, and southerly flow to push northward (Fig. 11f). This pattern of an upper-level trough and associated 850-hPa leeside troughing being present for less than 48 h was similarly observed during the shorter-duration SALLJ events when the jet also generally peaked in the low levels overnight. In these scenarios, lee

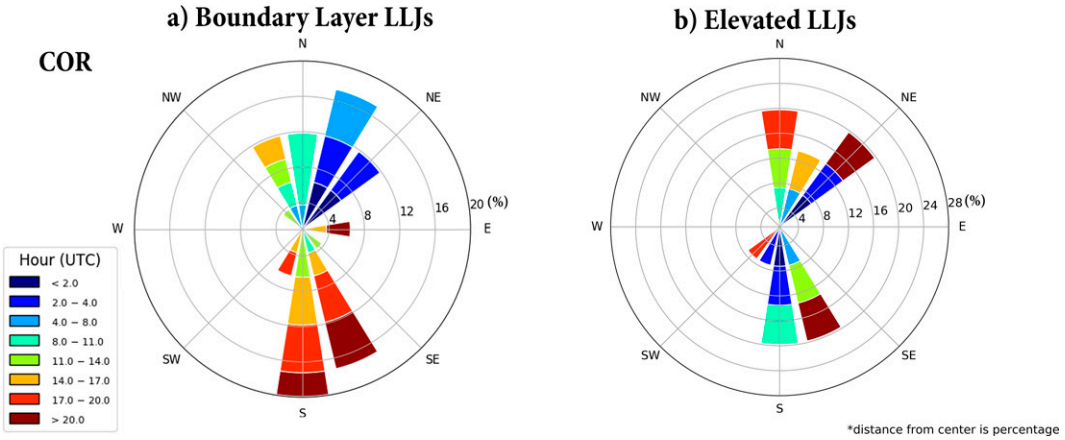

FIG. 10. Diurnal cycle of winds at 900 hPa for COR for all soundings during (a) four boundary layer LLJ days and (b) elevated LLJ days. The boundary layer LLJ days included are 5, 17, 22, and 26 Nov 2018. The elevated days are 12 Nov and 13 Dec 2018.

cyclogenesis, often with an accompanying frontal passage, appeared to influence the low-level flow. As mentioned earlier, frontal passages were not always easily identifiable in the shorter-duration events as surface-based features tended to be mixed out due to the strong surface heating. Unique to the 19–22 November event was an extension of the subtropical high over the Atlantic during 19–20 November (Figs. 11a,b) that also led to a boundary layer LLJ (Figs. 3 and 4), thus extending the duration of the northerly flow prior to the passage of the upper-level trough. Large-scale analysis, from this case, combined with the diurnal plots (Figs. 9a,b and 10a) suggests that a boundary layer SALLJ can occur under the combined influences of diurnal processes and the passage of an upper-level trough.

The 5–6-day SALLJ events were similar to the shorter-duration events described above in that the jet occurrence was linked to the passage of an upper-level trough. For the 8–12 November event, synoptic maps in Fig. 12 show one upper-level trough during this period, moving much more slowly across the region compared to the shorter-duration SALLJ events (e.g., Fig. 11) that results in an extended duration of low-level northerly flow (as also shown in Figs. 3, 4 and 8). Piersante et al. (2021) found that the 500-hPa trough over the Pacific slows and actually stalls at one point on 11 November. The high pressure over the Atlantic Ocean is shifted farther to the east compared to many of the shorter-duration SALLJ events, suggesting that the high plays less of a role in the strengthening of the SALLJ than the 850-hPa lee troughing for the 8–12 November event (Fig. 12). Near the end of the event on 11 November, shallow low-level flow switched from northerly to southerly before becoming deeper by 13 November (Figs. 3 and 4). This switch was preceded by the LLJ core winds receding northward (Fig. 8). Northerly winds occurred farthest south on 8 November (mostly south of the latitudes of COR and VMRS; shown by the gray dashed lines in Fig. 8), but by 12 November the core of the northerly low-level winds was north of COR and VMRS. This timing aligned with the leeside 850-hPa low shifting north then eastward (Fig. 12; Piersante et al. 2021) along with a frontal boundary (based on SMN analysis) passing through COR around 0000 UTC 11 November. During this SALLJ event, northerly flow was continuously present over a period of five days and coincident with the slow and sometimes stagnated upper-level trough, consistent with prior results from Rasmussen and Houze (2016).

Differing from the 8–12 November event, the extended period of strong northerly flow during 8–13 December was linked to multiple, closely spaced troughs. Similar to the shorter-duration SALLJ events, upper-level disturbances passing over the Andes induced 850-hPa lee troughs during 8–13 December (Fig. 13), but the pattern progressed slightly more slowly than the shorter-duration SALLJ events, and, more notably, three 500-hPa troughs moved through in very close succession (numbered on Fig. 13). The close spacing between these troughs meant that any gaps in northerly flow were brief, if present at all (Figs. 3, 4, and 8). The three periods of strong northerly flow are consistent in timing with the three troughs traversing the area in close succession. Overall, we infer from this analysis that the duration of the SALLJ events near the SDC is strongly linked with the upper-level pattern. Furthermore, a switch to southerly low-level flow at the end of the event results from the propagation of the pattern northward than eastward as discussed for the 8–12 November event in Piersante et al. (2021).

To link the apparent leeside troughing resulting from the passage of upper-level troughs to the SALLJ, the 850-hPa east–west height difference is computed over the area where troughing was most often present downstream of the Andes and the SALLJ occurred (Fig. 14). Because of the sharpness of the lee trough (seen in map in Fig. 14b), it was determined that an east–west height difference was best suited to determine the trough strength. An east–west height difference was present during all of the SALLJ events, but the greatest differences were found during the two 5–6-day SALLJ events (dark gray boxes; Fig. 14a). During the 8–12 November event,

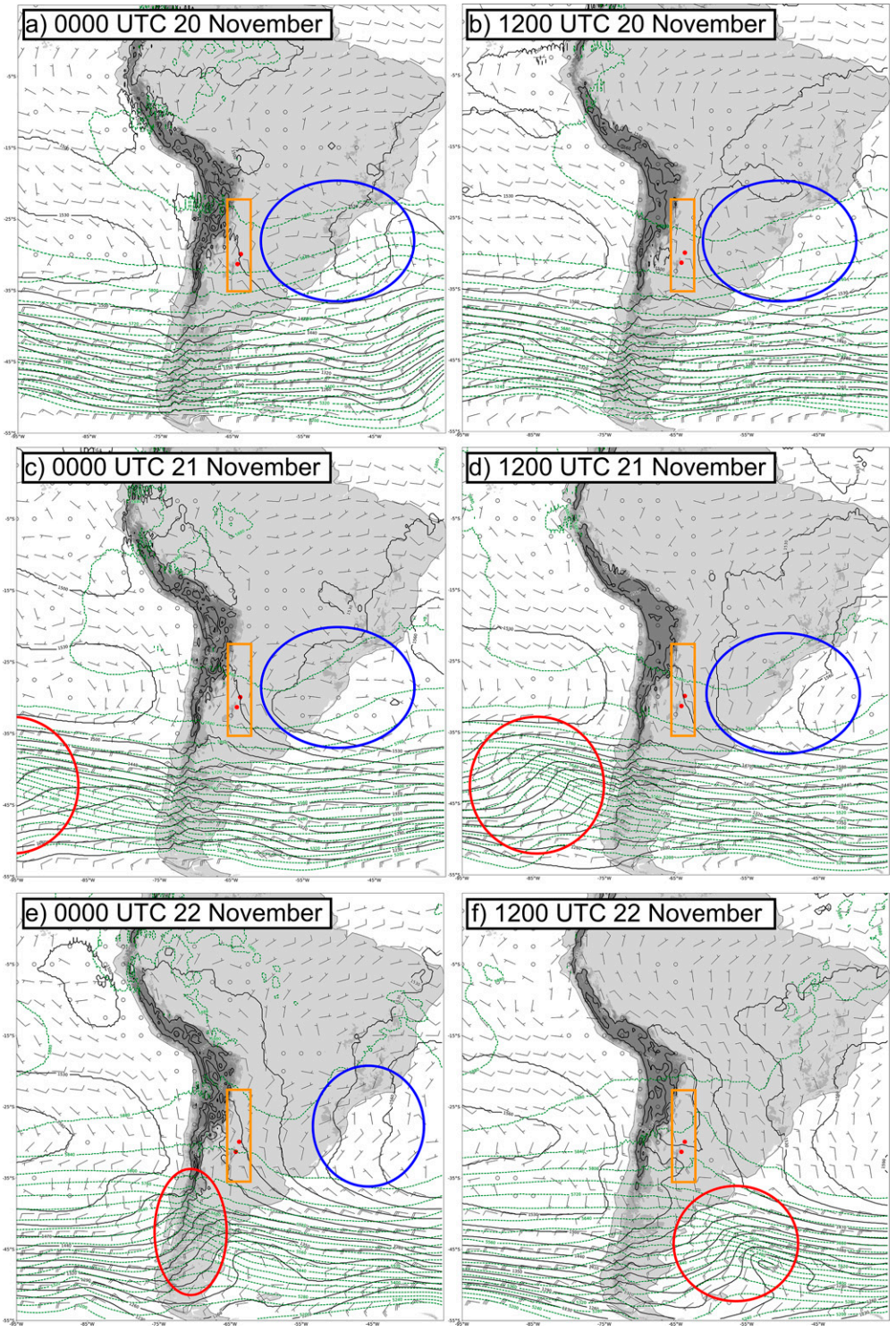

FIG. 11. Synoptic maps from ERA5 data for the 19–22 Nov 2018 event when a shorter-duration LLJ was observed at COR and VMRS: (a) 0000 UTC 20 Nov, (b) 1200 UTC 20 Nov, (c) 0000 UTC 21 Nov, (d) 1200 UTC 21 Nov, (e) 0000 UTC 22 Nov, and (f) 1200 UTC 22 Nov. Terrain is shown in the shaded grayscale colors. The two red dots indicate the locations of VMRS and COR. The black solid contours and black wind barbs show 850-hPa heights and winds, respectively. The green dashed lines show 500-hPa heights. The red circles highlight the position of the upper-level shortwave. The blue circles highlight the extension of the high pressure centered over the Atlantic Ocean. The orange boxes highlight the region of northerly flow near the SDCs.

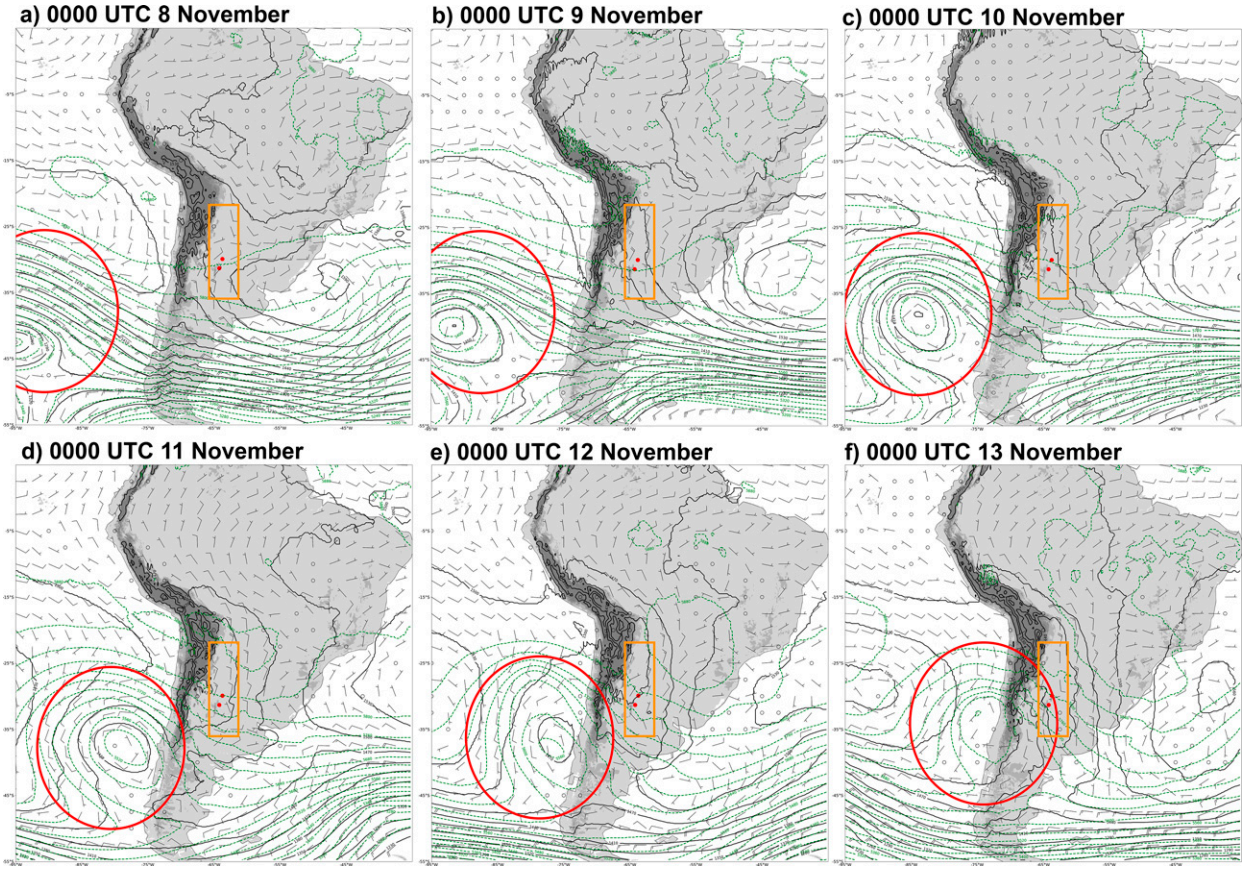

FIG. 12. As in Fig. 11, but daily synoptic maps at 0000 UTC for the 8–12 Nov 2018 event when a 5–6-day SALLJ was observed at COR and VMRS. One slow-moving, upper-level trough is highlighted by the red circles.

the height difference increased in strength as the trough slowly moved through the area. During the 8–13 December event there are three clear increases in the strength of the height difference which match well with the strongest times of northerly flow from Fig. 8. The 4–5 November and 26 November SALLJ events have the weakest height differences of the shorter-duration events (light gray shaded; Fig. 14a) and also have the weakest northerly flow at COR/VMRS (Fig. 8). This relationship suggests that the strength of the 850-hPa trough is related to the strength of the SALLJ and therefore connects the elevated LLJ occurrence to the passage of upper-level disturbances beyond ageostrophic circulations for the events analyzed. This result is consistent with composite model-based analyses from Rasmussen and Houze (2016) showing that the SALLJ increased in magnitude as the 850-hPa height difference strengthened associated with lee cyclogenesis processes. Additionally, the large height differences on the last days of 5–6-day SALLJ events (Fig. 14a) followed by the north and eastward movement of the 850-hPa lee low (discussed earlier) may have resulted in the elevated jets on those days.

Ultimately, we are interested in the influence the SALLJ has on the environmental conditions favoring convection, with studies suggesting the transport of warm, moist air from the Amazon to the SDC region via the jet. Therefore, we start with the HYSPLIT model (Stein et al. 2015) to examine the source regions and vertical motion history of the air that arrives at VMRS and COR through creating 72-h backward trajectories at those two stations. Figure 15 shows these trajectories for the two 5–6-day events (8–12 November, 8–13 December; Fig. 15a), the 21–22 November event that represents the pattern of most shorter-duration events (Fig. 15b), and the 16–17 December event that varies slightly from the other short-duration events (Fig. 15c). Air parcels that ended at 500 hPa at VMRS and COR (green) originated from the Pacific Ocean and crossed the Andes at similar locations for all events (Figs. 15a–c).

The largest differences between the shorter-duration and 5–6-day events (Figs. 15a–c) are found in the trajectories for air parcels ending at 850 hPa (red). In the shorter-duration events (represented by 21–22 November and 16–17 December), the 850-hPa trajectories originated at a similar latitude to where they ended, recycling air from the region (Figs. 15b,c). While there is variability in the exact path for all shorter-duration events, the 850-hPa trajectories stayed south of Bolivia with the majority curving around within Argentina. Comparatively, for the 5–6-day events the low-level air originated from areas farther north with the air originating from the Amazon around 12°S during the December event (Fig. 15a).

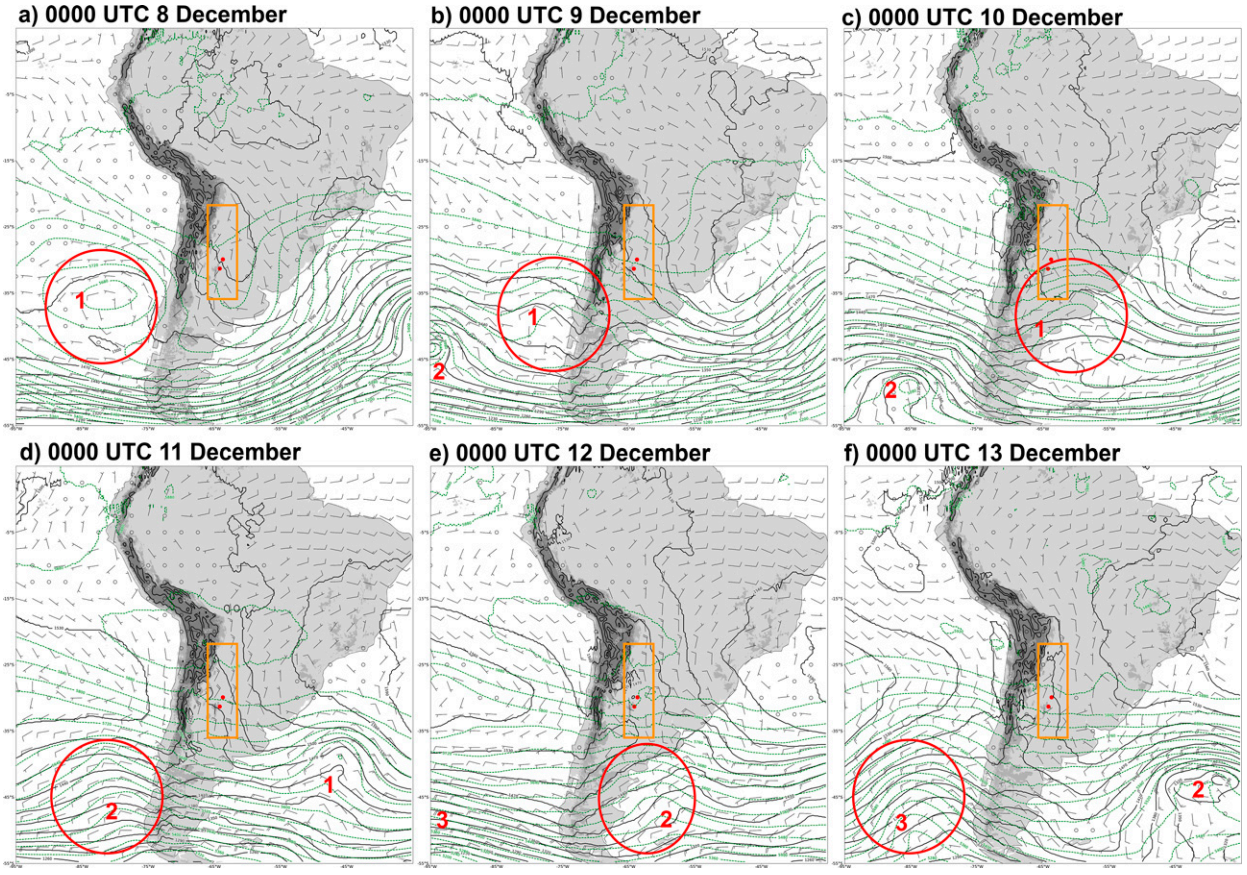

FIG. 13. As in Fig. 11, but daily synoptic maps at 0000 UTC for the 8–13 Dec 2018 event when a 5–6-day SALLJ was observed at COR and VMRS. Three upper-level shortwaves are labeled using numbers.

Trajectory pathways for air parcels ending at 700 hPa (blue) also illustrate differences between the shorter-duration and 5–6-day events. For the two 5–6-day SALLJ events these pathways were similar to those ending at 500 hPa; they originated over the Pacific and crossed over the Andes (Fig. 15a). Air parcels in the 5–6-day events experienced strong subsidence when they crossed the Andes, descending over 3000 m in less than 6 h (Figs. 15d,e). Contrastingly, for most of the shorter-duration events, the trajectories at 700-hPa traced a counterclockwise pattern over northeast Argentina/Paraguay and, similarly to 850-hPa, they stayed south of Bolivia. This pattern is exemplified by the 21–22 November event (Fig. 15b). The air parcels experienced little vertical motion and any change in height was gradual (Fig. 15f). The 16–17 December event differed from the other shorter-duration events at 700-hPa (blue). The 700-hPa trajectories on 17 December (Fig. 15c) split with one tracing back over the Andes and other from farther north. The trajectory crossing the Andes experienced some subsidence while the other one does not (Fig. 15g). The 16–17 December event is the only shorter-duration event that differs at 700-hPa and it is consistent with the other shorter-duration events at 850 and 500 hPa.

Overall, the differences between the shorter-duration and 5–6-day events appear in the mid and low-level airstreams. During the 5–6-day events, strong subsidence over the Andes reached into the midlevels and the spatial extent of the low-level trajectories was larger, particularly originating farther north. These differences have impacts on the moisture availability and convective coverage in the SDC region.

d. SALLJ impacts on moisture availability and the presence of convection

A northward origin of the 850-hPa trajectories appeared to be linked with higher moisture availability in the SDC region (Fig. 15). Specifically, the 5–6-day events featured prolonged periods of higher amounts of moisture (as measured by specific humidity) at 850 hPa and moisture extending farther south, as compared to the shorter-duration events.

Warmer temperatures and higher amounts of moisture were found at the origin of the 5–6-day event trajectories compared to the origin of most of the shorter-duration events (Figs. 15a,b). Additionally, when the air passed over Northern Argentina, the 850-hPa trajectories from the 5–6-day events still had a higher amount of moisture than those from most of the shorter-duration events (e.g., ~12 g kg^{-1} for 10 November versus 9–10 g kg^{-1} for 21 November; Figs. 15a,b). This suggests that the 5–6-day events may have established links with tropical moisture over the Amazon. Conversely, the shorter

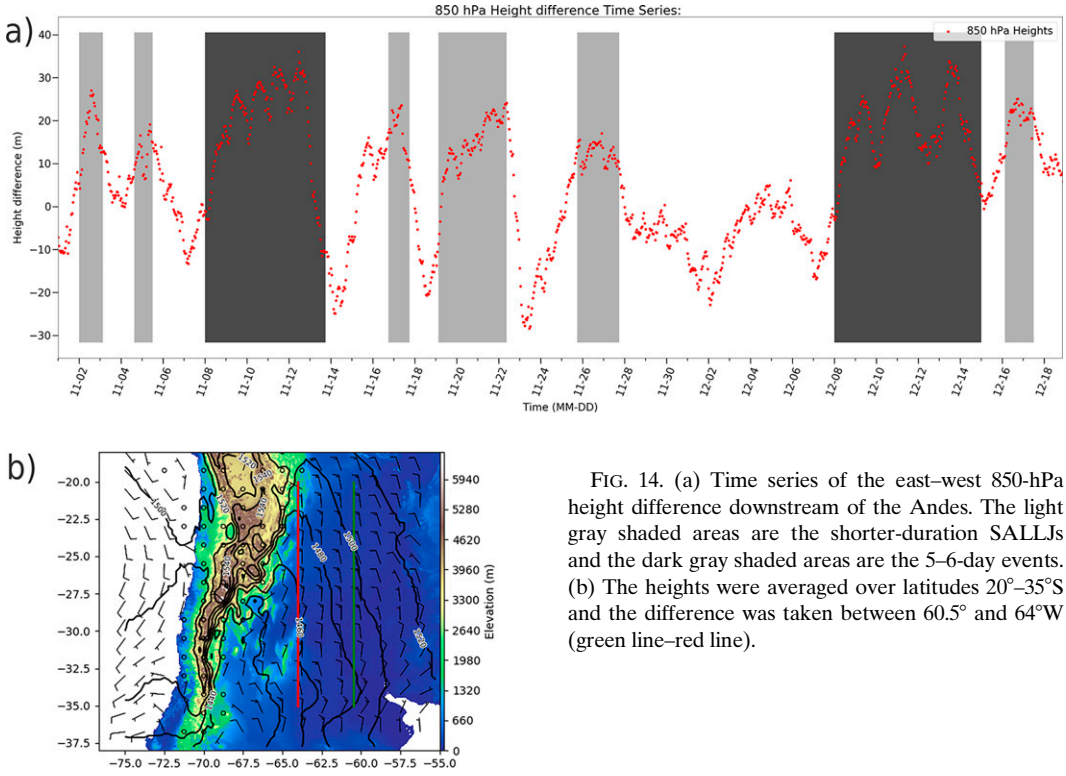

FIG. 14. (a) Time series of the east–west 850-hPa height difference downstream of the Andes. The light gray shaded areas are the shorter-duration SALLJs and the dark gray shaded areas are the 5–6-day events. (b) The heights were averaged over latitudes 20°–35°S and the difference was taken between 60.5° and 64°W (green line–red line).

northward latitudinal extent at 850 hPa in the shorter-duration events correlates with less moisture, with the exception of the 16–17 December event to be discussed in the next section.

The influence of the different 850-hPa airstreams is evident from a north–south Hovmöller of 850-hPa specific humidity produced using ERA5 data (Fig. 16). The v winds greater than 20 kt (1 kt = 0.51 m s^{-1}) are overlaid with northerly and southerly winds represented by dashed and solid lines, respectively. Specific humidity was greater (>10 g kg^{-1}) at the latitudes of VMRS and COR (gray dashed lines) around the times of strong northerly flow (dashed lines). During the two 5–6-day SALLJ events in the black boxes, greater specific humidity was present for extended periods (>3 days) and specific humidity was higher (13–16 g kg^{-1}) than many of the shorter-duration events. This observation is particularly apparent near the end of these events when the highest specific humidity values occurred. Furthermore, specific humidity extended farther south, with >10 g kg^{-1} reaching 35°S, and was deeper at 35°S during the 5–6-day events than in the shorter-duration events. These time periods coincided with the longest duration northerly flow and where the 850-hPa flow was traced to areas farther north (Fig. 15a). The higher amounts of specific humidity are consistent with a connection to the Amazon as the moisture source and the longest duration of northerly flow. The shorter-duration SALLJ on 16–17 December is an exception to the pattern of specific humidity being more limited south of the SDC region during the shorter-duration events. However, this event follows the December 5–6-day event and higher amounts of moisture persist past the cessation of the jet north of COR/VMRS, even as the study area dries out (Fig. 16). The shorter-duration SALLJ on 16–17 December is therefore likely able to transport higher amounts of moisture southward, from just north of COR/VMRS, without low-level flow originating from as far north as the two longer-duration events (Fig. 15c).

Convective coverage was calculated as the area downstream of the SDC with *GOES-16* IR temperatures less than 235 K (Fig. 17). Northerly SALLJ events are shaded with shorter events in light gray and the 5–6-day events in dark gray. These SALLJ events that had increased moisture (specific humidity > 10 g kg^{-1}, Fig. 16), were also concurrent with times of extensive convection downstream of the SDC (Fig. 17). Within each event, convective coverage tended to peak near the end or just after the period of strongest northerly flow. This timing could be the result of frontal passages associated with the progression of the pattern passing through the area acting as a lifting mechanism. The rapid growth of convection after these frontal passages may be caused by a combination of impacts of the SALLJ including continued moisture transport, thermodynamic destabilization, vertical wind shear, and low-level convergence. The highest convective coverage occurred during the two 5–6-day SALLJ events when about half to three quarters of the area was covered. Convection was also widespread during the short SALLJ event on 17 December. The highest levels of moisture were concurrent with the times of highest convective coverage

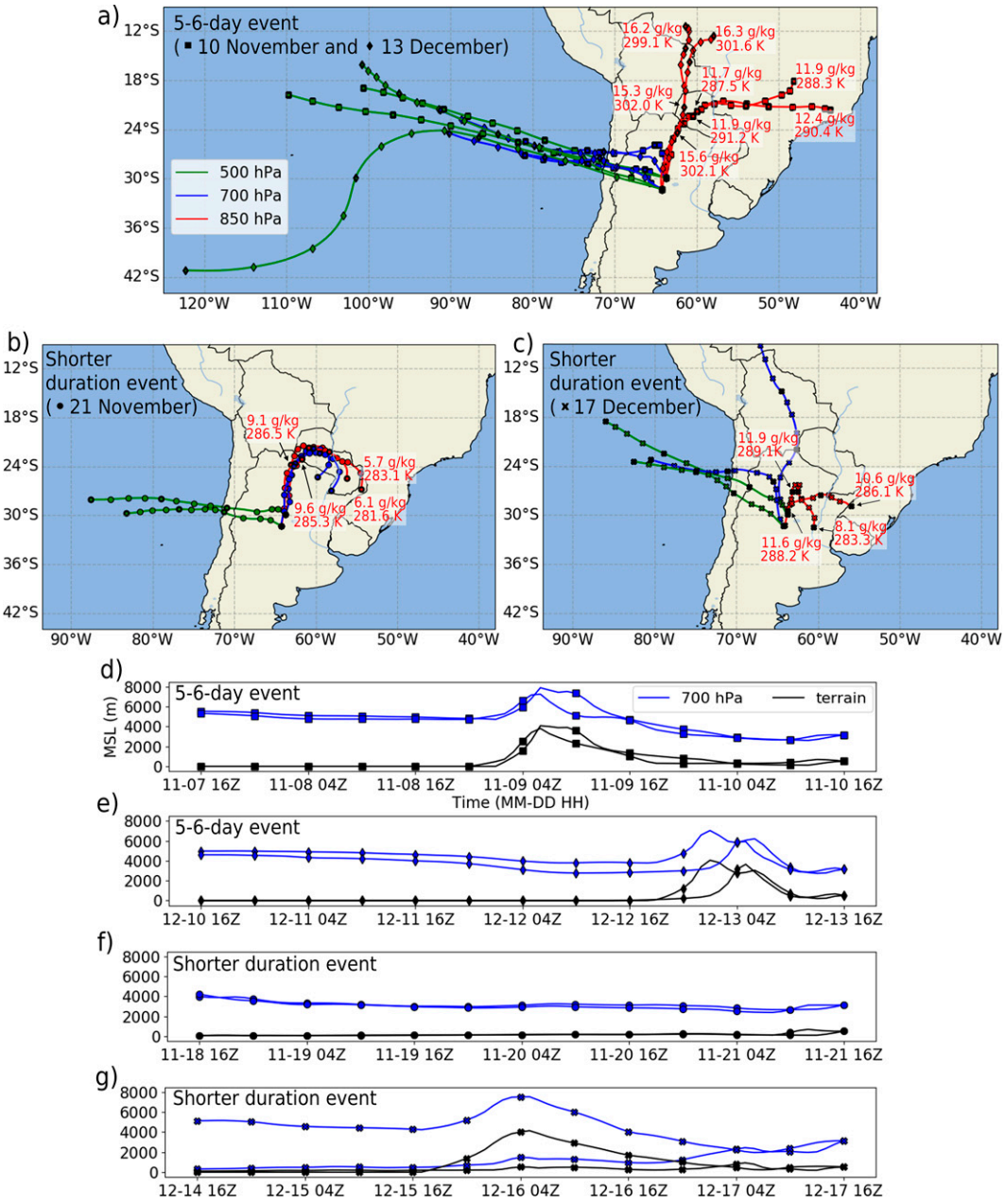

FIG. 15. The 72-h backward trajectories at COR and VMRS from the HYSPLIT model ending at 1600 UTC for four SALLJ events: (a),(d) 10 Nov; (a),(e) 13 Dec; (b),(f) 21 Nov; and (c),(g) 17 Dec. The shape of the point corresponds to each event: square (10 Nov), diamond (13 Dec), circle (21 Nov), and × (17 Dec). Points are plotted every 6 h and the bolded points are every 24 h. The colors indicate ending height: 850 (red), 700 (blue), and 500 hPa (green). The maps in (a)–(c) show the horizontal tracks with the bottom plots in (d)–(g) showing the vertical movement of air through time for trajectories ending at 700 hPa. The black lines in (d)–(g) show the terrain height along the trajectory. The red numbers in (a)–(c) are 850-hPa specific humidity and air temperature.

(Fig. 16), but additional factors discussed above might also be increased due to the longevity of the SALLJ. Moisture is only one ingredient necessary for convection and the connection between the SALLJ and the convective environment must be further investigated through RELAMPAGO observations.

4. Discussion

Our findings are broadly consistent with past studies of the SALLJ and its connection with convective storms in subtropical South America. The shorter-duration events observed during RELAMPAGO share characteristics with NLLJs such

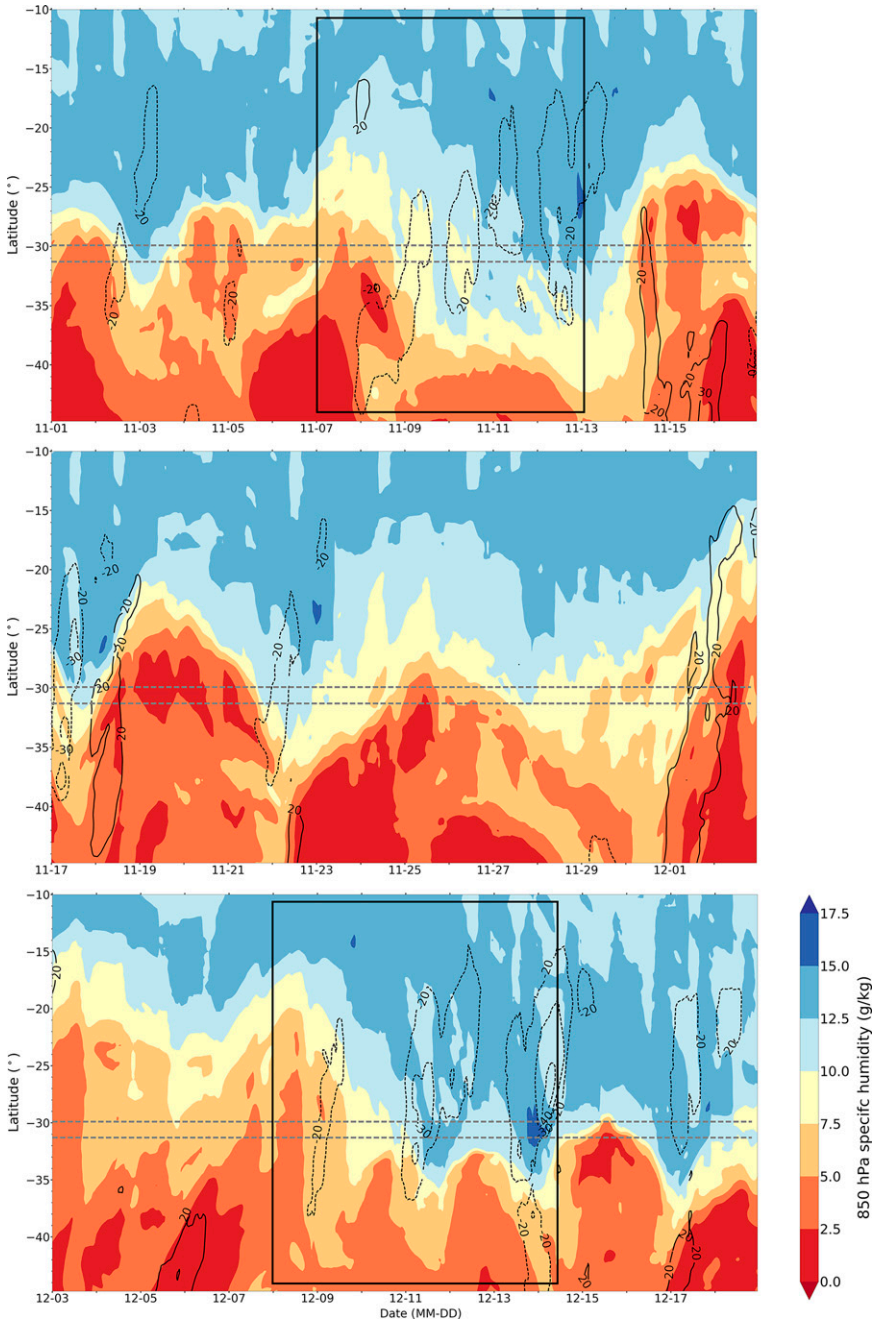

FIG. 16. North–south Hovmöller diagram of 850-hPa specific humidity (shaded) and v wind > 20 kt (dashed contours from north, solid from south) averaged over 55° to 65°W using ERA5. Dash–dotted lines show the latitude of VMRS (northern) and COR (southern). The black boxes are the two 5–6-day northerly SALLJ events from the observational plots.

as an overnight peak in intensity and counterclockwise wind gyre and with previous analyses of the SALLJ using SALLJEX observations (Vera et al. 2006; Nicolini et al. 2004a), reanalysis data (e.g., Marengo et al. 2004), and model output (e.g., Nicolini and Saulo 2006). These shorter-duration events were observed most frequently in our analysis and therefore likely represent the mean SALLJ (e.g., Salio et al. 2002); however, RELAMPAGO observations (Figs. 6b,e) verified that the height of jet cores varied quite widely including elevated jets with cores peaking up to 650 hPa (e.g., ONK18) that occurred near the end of the two 5–6-day SALLJ events. Peak intensity of these elevated jets did not follow a diurnal cycle, thus resembling a LLJS rather than a NLLJ. The distinct characteristics of the jets during these 5–6-day events, from those during the shorter-duration events,

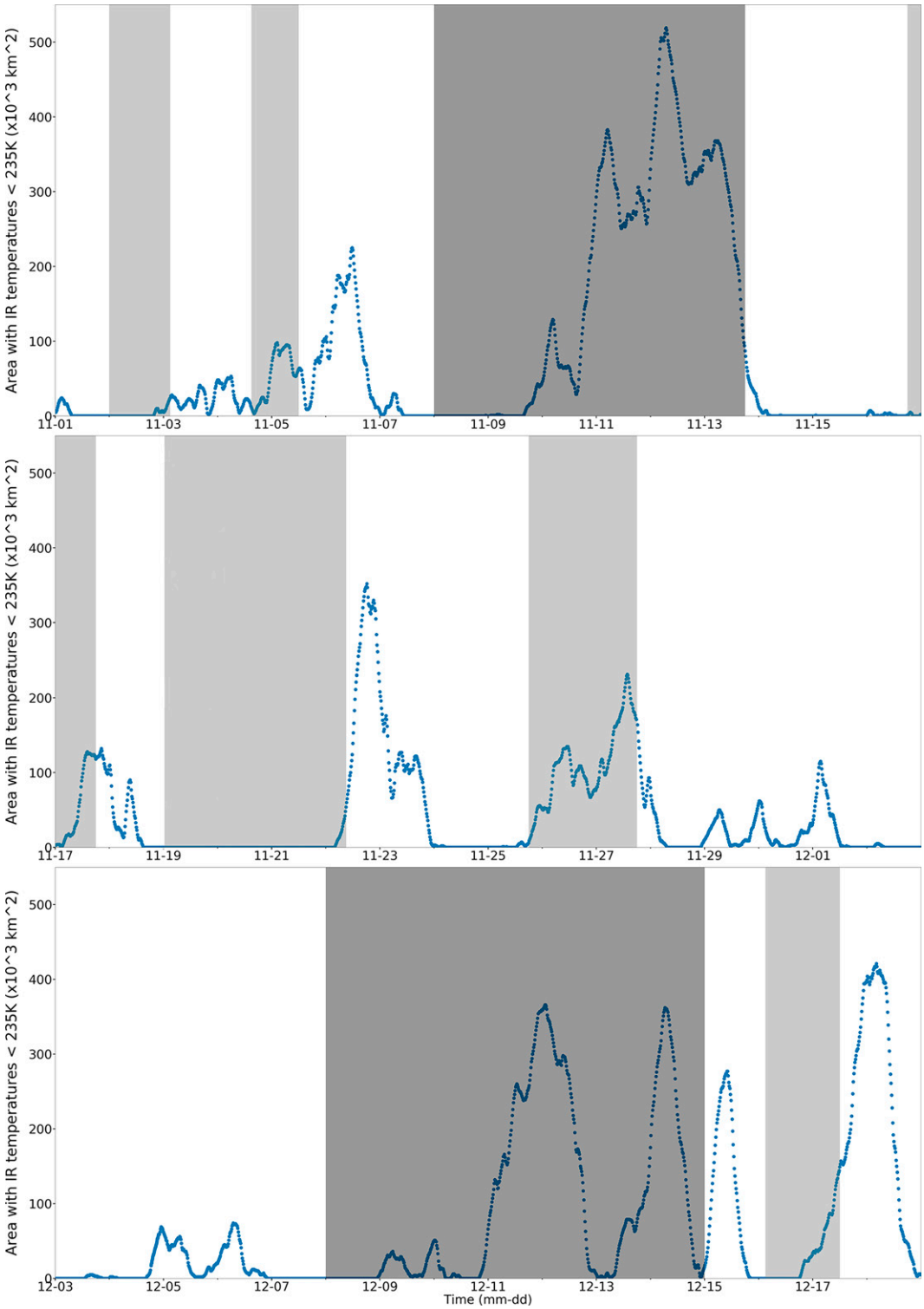

FIG. 17. Time series of area with *GOES-16* IR temperatures less than 235 K. The region used (29°–35°S, 55°–66°W) was an area downstream of the SDC (black box Fig. 1). The total area of the region is about 690 000 km^2. The light gray shaded areas represent the shorter-duration northerly SALLJs with the dark gray shaded areas being the 5–6-day events.

motivated a closer look at the mechanisms driving the SALLJ and their impact on SALLJ characteristics.

Our analysis revealed the presence of synoptic forcing in all RELAMPAGO SALLJ events, as evidenced by upper-level troughs traversing the Andes followed by the presence of lee cyclogenesis and subsidence. Our finding that the greatest east–west height differences at 850 and 700 hPa occurred during identified SALLJ events along with upper-level disturbances is consistent with lee cyclogenesis playing an important role in the analyzed SALLJ events (e.g., Rasmussen and Houze 2016). Large-scale analysis, combined with diurnal plots, suggests that boundary layer SALLJs occur under the combined influences of diurnal processes and the passage of an upper-level trough. Compared to the United States, the lack of gentle sloping terrain, extreme height of the Andes, and increased frequency of summertime synoptic activity (Garreaud and Wallace 1998) could explain the increased importance of synoptic disturbances to instances of the SALLJ.

Our results showed the combined influence of the leeside low and South Atlantic subtropical high on creating the gradient that extends the SALLJ down into Argentina, as hypothesized in composites from Nicolini et al. (2004b). Expanding upon that previous work, this study found that lee troughing appeared to be more influential to the magnitude of the gradients than the South Atlantic subtropical high during the two 5–6-day SALLJ events analyzed, particularly during the 8–12 November event. This result could be explained by the unseasonably strong upper-level trough identified by Piersante et al. (2021). During the shorter-duration events, high pressure acted to strengthen the low-level gradient, especially when the upper-level trough (and corresponding lee troughing) was weaker than in the 5–6-day events or located farther south of the RELAMPAGO domain.

Overall, our analysis suggests the duration of SALLJ events is broadly tied to the upper-level pattern. Progressive patterns with spaced out troughs coincided with shorter-duration SALLJs while closely spaced or quasi-stationary troughs coincided with the 5–6-day SALLJ events. In the case of the 19–22 November event, the duration of the SALLJ was extended prior to the passage of the upper-level trough by a preexisting low-level gradient resulting from an extension of the subtropical high. We further tied periods of extended synoptic activity to the 5–6-day SALLJ events through the presence of deep-layer subsidence, providing evidence for hypotheses from previous studies on the relationship between subsidence and the strengthening of the lee low (e.g., Seluchi et al. 2003; Rasmussen and Houze 2011). This pattern likely contributed to the strong 850-hPa height gradients (Fig. 14) that were coincident with low-level southerly flow on the backside of lee cyclones and may have resulted in the elevated LLJs near the end of the 5–6-day SALLJ events (e.g., Saulo et al. 2004; ONK18).

This study examined the relationship between the SALLJ, moisture transport, and convection near the SDC. Our findings suggest that the Amazon is the moisture source during our two 5–6-day events (Figs. 12 and 13), as shown in prior reanalysis studies (e.g., Nogués-Paegle and Mo 1997); however, low-level air does not appear to be transported from as far north in the shorter-duration events (Fig. 11), suggesting a different moisture source. The moisture in the shorter-duration events being fed by local moisture recycling (Martinez and Dominguez 2014) aligns with the slightly lower amounts of moisture observed in reanalysis data that may influence the impact of the SALLJ on convection (e.g., Saulo et al. 2007; Salio et al. 2007; Borque et al. 2010), which is a focus of future work.

5. Conclusions

This study builds on prior research by explaining a typology of the SALLJ based on observations, provides more evidence of its drivers, and infers initial links to widespread convection near the SDC. Using high temporal soundings obtained during RELAMPAGO along with ERA5 data, we examine the variability and characteristics of the SALLJ in central Argentina during this campaign and found jets of varying height (boundary layer and elevated LLJs) and varying durations (<2 up to 6 days). Our primary results are summarized as follows:

- The shorter-duration SALLJ events were the most frequent SALLJ events during RELAMPAGO and had characteristics resembling those of a NLLJ, including intensity peaking overnight at or below 825 hPa. Two 5–6-day SALLJ events were observed during RELAMPAGO ending with persistent, elevated LLJs (i.e., peaking above 825 hPa) that resembled LLJS with little connection to the diurnal cycle.
- Evidence was found for the influence of synoptic-scale processes for all SALLJ events during RELAMPAGO with upper-level troughs and associated lee cyclogenesis near the SDC. The upper-level pattern was progressive during the shorter-duration events, whereas quasi-stationary or upper-level troughs moving through the area in close succession produced extended periods of lee cyclogenesis with stronger east–west pressure gradients during 5–6-day SALLJ events.
- Direct moisture transport from the Amazon may be a unique feature of the longest 5–6-day SALLJ events. The availability of ample moisture and/or the increased duration of moisture transport may be responsible for increasing the environmental moisture southward into central Argentina, especially near the SDC. In the shorter-duration events, moisture did not appear to originate from as far north, possibly partly explaining the slightly lower amounts of moisture present.
- The most widespread convection occurred near the end or just after SALLJ events, with greatest coverage at the end of 5–6-day SALLJ events when the jet was most elevated and high amounts of moisture were present.

These findings will enable future research to understand the stages in the convective life cycle in which the SALLJ has an influential role. This study was able to identify specific characteristics of 5–6-day SALLJ events during times of

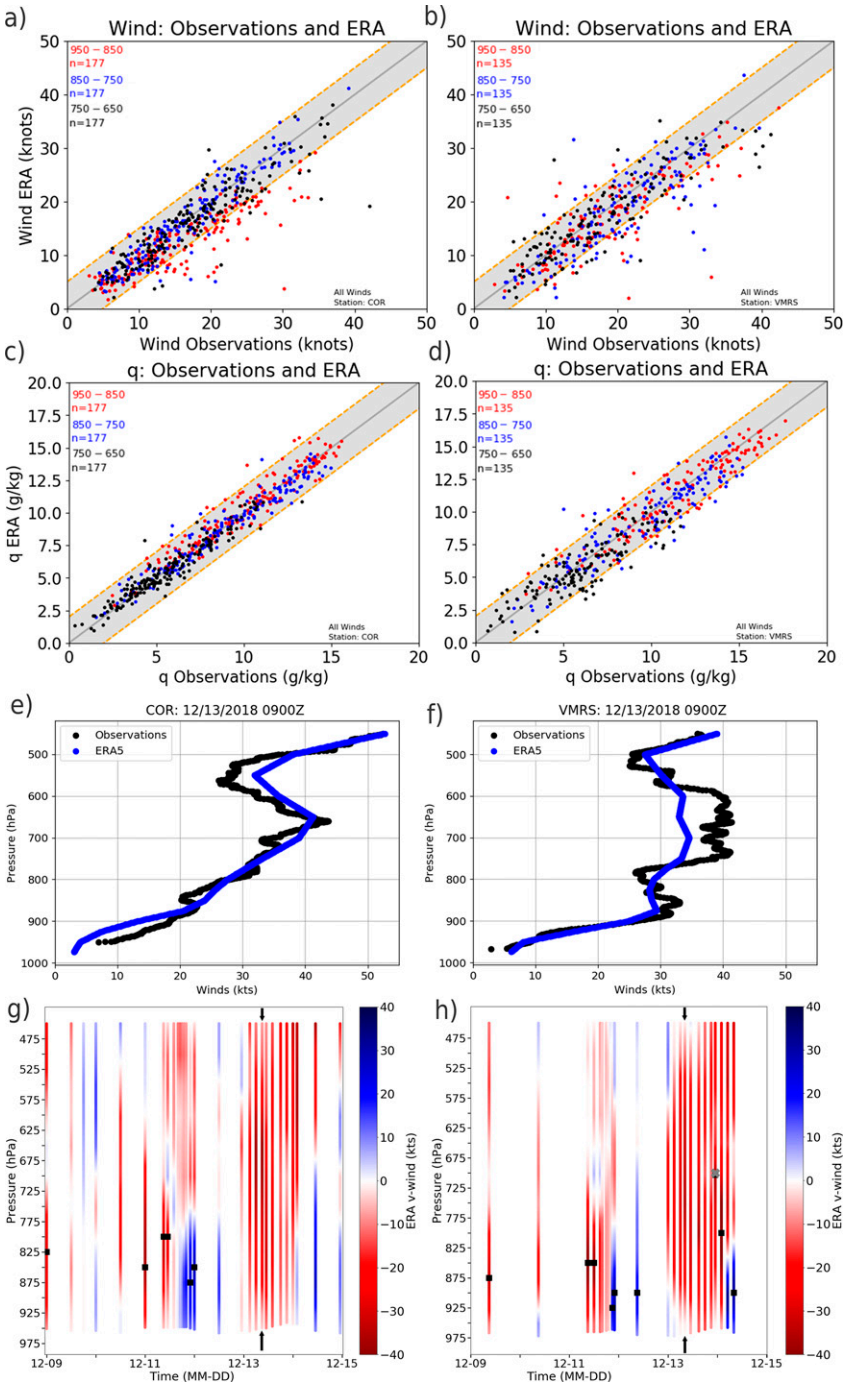

FIG. A1. Comparison of (a),(b) mean-layer wind speeds and (c),(d) specific humidity in ERA5 data and observational soundings. The value found in the ERA5 dataset is on the y axis and the value observed from soundings is on the x axis. Color indicates the layer over which the mean is taken, with red for 950–850 hPa, blue for 850–750 hPa, and black for 750–650 hPa. The gray solid line indicates the same value in ERA5 as in observations and the orange dashed lines are (a),(b) ±5 kt for wind speeds and (c),(d) ±2 g kg^{-1} for specific humidity. (e),(f) Comparisons of ERA5 and observational vertical wind profiles from 0900 UTC 13 Dec. (g),(h) ERA5 v-wind sounding time series for 9–14 Dec using the same times that observational soundings were launched. The v component of the wind from the north (red) and from the south (blue). The level of maximum wind (jet core) is shown for soundings with a LLJ identified from Oliveira et al. (2018) criteria (black squares) and additional LLJs found when applying our modified criteria (gray × symbols). The arrows point to the vertical profile shown in (e),(f). (a),(c),(e),(g) COR and (b),(d),(f),(h) VMRS.

widespread convection which allows us to begin to test theories of synergism between the jet and convection (e.g., Saulo et al. 2007). One hypothesis is that the jet has a role in maintaining and organizing convection through continued moisture transport, enhanced low-level convergence, and the presence of strong vertical shear. Near the end of the 5–6-day events, the jet is elevated and features southerly undercutting flow, creating strong wind shear which we believe may aid in the rapid organization of convection (e.g., Piersante et al. 2021). With additional observations from mobile sounders and reanalysis available from the RELAMPAGO period, along with high-resolution model simulations during these convection events, future research will more closely examine the relationship of environmental characteristics produced by the jet (e.g., wind shear and low-level convergence), the terrain (e.g., subsidence), and the upper-level jet stream (e.g., upper-level divergence) with respect to the convective life cycle, including the relationship between the SDC, SALLJ flow patterns, and rapid upscale growth of convection.

Acknowledgments. The authors thank all the participants of the RELAMPAGO campaign for battling the elements to get the sounding data used in this study. Additional thanks go out to Stacy Brodzik for managing the data used and Jeremiah Piersante for providing helpful feedback. Thank you to the editor and anonymous reviewers for helping to improve the manuscript. This research was supported by NSF Grants AGS-1661768 and AGS-1661657.

Data availability statement. Quality controlled RELAMPAGO soundings and *GOES-16* data are available from the NCAR EOL online data archive (https://data.eol.ucar.edu/master_lists/generated/relampago/). ERA5 data are available through Copernicus (https://cds.climate.copernicus.eu/cdsapp#!/home).

APPENDIX

ERA5 Evaluation

While RELAMPAGO produced high-temporal ground-based observations in central Argentina, the observations were still limited in time and particularly in space. The observations provided 3-hourly soundings during IOPs allowing for the identification of SALLJ periods of varying duration. However, with the reduction of soundings outside of these IOPs, it is difficult to clearly determine the start and stop times of these enhanced periods of northerly flow. The hourly ERA5 dataset helps to fill in these temporal gaps. Further, station-based observational data are too limited for synoptic-scale analysis; therefore, ERA5 is necessary to understand the influence of the synoptic environment on the presence and evolution of the SALLJ.

To use ERA5 to analyze synoptic-scale flow and moisture patterns, ERA5 winds and moisture were evaluated against the COR and VMRS sounding data (Fig. A1). With respect to winds, at least 80% of the mean wind speeds over all the calculated layers fell within a 5-kt error compared to observations (Figs. A1a,b). The magnitudes of the errors were slightly smaller for the most elevated winds (750–650 hPa; black) than the lowest levels (950–850 hPa; red). The largest errors are found at COR in the lower levels along with a consistent low bias that is similar in magnitude to the errors. Overall, for our purposes in identifying periods of increased northerly flow over central Argentina, ERA5 captures the general flow pattern present in the observations. Using the 9–14 December event as an example, the evolution of winds in the ERA5 time series (Figs. A1g,h) is similar to those from observations (Figs. 3 and 4) at all heights and at both stations. Therefore, ERA5 can be used to interpolate between soundings and extend our analysis of winds in time and space.

Additionally, moisture is transported by SALLJs and is a necessary component of convection; therefore, it is important that the ERA5 correctly represents moisture for our efforts in evaluating the extent and magnitude of low-level moisture availability. At least 90% of the mean specific humidity values over all the calculated layers fell within a 2 g kg^{-1} error compared to observations (Figs. A1c,d). We believe this result indicates that specific humidity from ERA5 accurately represents the observed moisture patterns.

While the broad wind and moisture patterns from observations are found in ERA5, comparing specific soundings show important differences. The maximum and minimum wind found in observations is smoothed out in ERA5 data (Figs. A1e,f). Only about half of the LLJs found in the observed soundings were identified as LLJs in ERA5 (not shown). Prior research has documented similar challenges in capturing LLJs in reanalysis (e.g., Walters et al. 2014). Additionally, the switch to southerly winds occurs a little faster in ERA5 compared to observations (e.g., 0000 UTC 14 December at COR; Fig. A1g).

ERA5 reproduces the SALLJ events found from observations. Overall, the periods of enhanced northerly winds with increased moisture that match overall with the periods observed by the soundings. However, slight differences in timing and wind extrema limits using ERA5 data to explore details about specific timing and small-scale features. For these reasons, ERA5 data are not used for a detailed analysis of the SALLJ through objective identification in our study, but it is acceptable for describing the evolution of synoptic-scale wind and moisture patterns.

REFERENCES

Anabor, V., D. J. Stensrud, and O. L. L. De Moraes, 2008: Serial upstream-propagating mesoscale convective system events over southeastern South America. *Mon. Wea. Rev.*, **136**, 3087–3105, https://doi.org/10.1175/2007MWR2334.1.

Blackadar, A. K., 1957: Boundary layer wind maxima and their significance for the growth of nocturnal inversions. *Bull. Amer. Meteor. Soc.*, **38**, 283–290, https://doi.org/10.1175/1520-0477-38.5.283.

Bonner, W. D., 1968: Climatology of the low level jet. *Mon. Wea. Rev.*, **96**, 833–850, https://doi.org/10.1175/1520-0493(1968)096<0833:COTLLJ>2.0.CO;2.

Borque, P., P. Salio, M. Nicolini, and Y. G. Skabar, 2010: Environment associated with deep moist convection under SALLJ conditions: A case study. *Wea. Forecasting*, **25**, 970–984, https://doi.org/10.1175/2010WAF2222352.1.

Byerle, L. A., and J. Paegle, 2002: Description of the seasonal cycle of low-level flows flanking the Andes and their interannual variability. *Meteorologica*, **27**, 71–88.

Campetella, C. M., and C. S. Vera, 2002: The influence of the Andes Mountains on the South American low-level flow. *Geophys. Res. Lett.*, **29**, 6–9, https://doi.org/10.1029/2002GL015451.

Carril, A. F., and Coauthors, 2012: Performance of a multi-RCM ensemble for South Eastern South America. *Climate Dyn.*, **39**, 2747–2768, https://doi.org/10.1007/s00382-012-1573-z.

Carvalho, L. M. V., and C. Jones, 2001: A satellite method to identify structural properties of mesoscale convective systems based on the maximum spatial correlation tracking technique (MASCOTTE). *J. Appl. Meteor.*, **40**, 1683–1701, https://doi.org/10.1175/1520-0450(2001)040<1683:ASMTIS>2.0.CO;2.

Chen, Y.-L., X. A. Chen, and Y.-X. Zhang, 1994: A diagnostic study of the low-level jet during TAMEX IOP 5. *Mon. Wea. Rev.*, **122**, 2257–2284, https://doi.org/10.1175/1520-0493(1994)122<2257:ADSOTL>2.0.CO;2.

Du, Y., and R. Rotunno, 2014: A simple analytical model of the nocturnal low-level jet over the Great Plains of the United States. *J. Atmos. Sci.*, **71**, 3674–3683, https://doi.org/10.1175/JAS-D-14-0060.1.

——, Q. Zhang, Y. Ying, and Y. Yang, 2012: Characteristics of low-level jets in Shanghai during the 2008–2009 warm seasons as inferred from wind profiler radar data. *J. Meteor. Soc. Japan*, **90**, 891–903, https://doi.org/10.2151/jmsj.2012-603.

——, ——, Y. L. Chen, Y. Zhao, and X. Wang, 2014: Numerical simulations of spatial distributions and diurnal variations of low-level jets in China during early summer. *J. Climate*, **27**, 5747–5767, https://doi.org/10.1175/JCLI-D-13-00571.1.

Garreaud, R. D., and J. M. Wallace, 1998: Summertime incursions of midlatitude air into subtropical and tropical South America. *Mon. Wea. Rev.*, **126**, 2713–2733, https://doi.org/10.1175/1520-0493(1998)126<2713:SIOMAI>2.0.CO;2.

Hersbach, H., and Coauthors, 2020: The ERA5 global reanalysis. *Quart. J. Roy. Meteor. Soc.*, **146**, 1999–2049, https://doi.org/10.1002/qj.3803.

Hoecker, W., 1963: Three southerly low-level jet systems delineated by the Weather Bureau Special Pibal Network of 1961. *Mon. Wea. Rev.*, **91**, 573–582, https://doi.org/10.1175/1520-0493(1963)091<0573:TSLJSD>2.3.CO;2.

Holton, J. R., 1967: The diurnal boundary layer wind oscillation above sloping terrain. *Tellus*, **19**, 200–205, https://doi.org/10.3402/tellusa.v19i2.9766.

Houze, R. A., K. L. Rasmussen, M. D. Zuluaga, and S. R. Brodzik, 2015: The variable nature of convection in the tropics and subtropics: A legacy of 16 years of the tropical rainfall measuring mission satellite. *Rev. Geophys.*, **53**, 994–1021, https://doi.org/10.1002/2015RG000488.

Liu, C., and E. J. Zipser, 2015: The global distribution of largest, deepest, and most intense precipitation systems. *Geophys. Res. Lett.*, **42**, 3591–3595, https://doi.org/10.1002/2015GL063776.

Marengo, J. A., W. R. Soares, C. Saulo, and M. Nicolini, 2004: Climatology of the low-level jet east of the Andes as derived from the NCEP–NCAR reanalyses: Characteristics and temporal variability. *J. Climate*, **17**, 2261–2280, https://doi.org/10.1175/1520-0442(2004)017<2261:COTLJE>2.0.CO;2.

Martinez, J. A., and F. Dominguez, 2014: Sources of atmospheric moisture for the La Plata River basin. *J. Climate*, **27**, 6737–6753, https://doi.org/10.1175/JCLI-D-14-00022.1.

Matsudo, C. M., and P. V. Salio, 2011: Severe weather reports and proximity to deep convection over Northern Argentina. *Atmos. Res.*, **100**, 523–537, https://doi.org/10.1016/j.atmosres.2010.11.004.

Mezher, R. N., M. Doyle, and V. Barros, 2012: Climatology of hail in Argentina. *Atmos. Res.*, **114–115**, 70–82, https://doi.org/10.1016/j.atmosres.2012.05.020.

Montini, T. L., C. Jones, and L. M. V. Carvalho, 2019: The South American low-level jet: A new climatology, variability, and changes. *J. Geophys. Res. Atmos.*, **124**, 1200–1218, https://doi.org/10.1029/2018JD029634.

Mulholland, J. P., S. W. Nesbitt, R. J. Trapp, K. L. Rasmussen, and P. V. Salio, 2018: Convective storm life cycle and environments near the Sierras de Córdoba, Argentina. *Mon. Wea. Rev.*, **146**, 2541–2557, https://doi.org/10.1175/MWR-D-18-0081.1.

Nascimento, M. G., D. L. Herdies, and D. O. De Souza, 2016: The South American water balance: The influence of low-level jets. *J. Climate*, **29**, 1429–1449, https://doi.org/10.1175/JCLI-D-15-0065.1.

Nesbitt, S. W., R. Cifelli, and S. A. Rutledge, 2006: Storm morphology and rainfall characteristics of TRMM precipitation features. *Mon. Wea. Rev.*, **134**, 2702–2721, https://doi.org/10.1175/MWR3200.1.

——, and Coauthors, 2021: A storm safari in subtropical South America: Proyecto RELAMPAGO. *Bull. Amer. Meteor. Soc.*, **102**, E1621–E1644, https://doi.org/10.1175/BAMS-D-20-0029.1.

Nicolini, M., and A. C. Saulo, 2000: ETA characterization of the 1997–1998 warm season Chaco jet cases. Preprints, *Sixth Int. Conf. on Southern Hemisphere Meteorology and Oceanography*, Santiago, Chile, Amer. Meteor. Soc., 330–331.

——, and ——, 2006: Modeled Chaco low-level jets and related precipitation patterns during the 1997–1998 warm season. *Meteor. Atmos. Phys.*, **94**, 129–143, https://doi.org/10.1007/s00703-006-0186-7.

——, P. Salio, G. Ulke, J. Marengo, M. Douglas, J. Paegle, and E. Zipser, 2004a: South American low-level jet diurnal cycle and three dimensional structure. *CLIVAR Exchanges*, No. 9, International CLIVAR Project Office, Southampton, United Kingdom, 6–8.

——, ——, and J. Paegle, 2004b: Diurnal wind cycle of the South American low-level jet. *First Int. CLIVAR Science Conf. Poster Session 2: Monsoon Systems*, Baltimore, MD, WCRP, MS-80.

Nogués-Paegle, J., and K. C. Mo, 1997: Alternating wet and dry conditions over South America during summer. *Mon. Wea. Rev.*, **125**, 279–291, https://doi.org/10.1175/1520-0493(1997)125<0279:AWADCO>2.0.CO;2.

Oliveira, M. I., E. L. Nascimento, and C. Kannenberg, 2018: A new look at the identification of low-level jets in South America. *Mon. Wea. Rev.*, **146**, 2315–2334, https://doi.org/10.1175/MWR-D-17-0237.1.

Paegle, J., 1998: A comparative review of South American low level jets. *Meteorologica*, **23**, 73–81.

Piersante, J. O., K. L. Rasmussen, R. S. Schumacher, A. K. Rowe, and L. A. McMurdie, 2021: A synoptic evolution comparison of the smallest and largest MCSs in subtropical South America between spring and summer. *Mon. Wea. Rev.*, **149**, 1943–1966, https://doi.org/10.1175/MWR-D-20-0208.1.

Rasmussen, K. L., and R. A. Houze, 2011: Orogenic convection in subtropical South America as seen by the TRMM satellite. *Mon. Wea. Rev.*, **139**, 2399–2420, https://doi.org/10.1175/MWR-D-10-05006.1.

——, and ——, 2016: Convective initiation near the Andes in subtropical South America. *Mon. Wea. Rev.*, **144**, 2351–2374, https://doi.org/10.1175/MWR-D-15-0058.1.

——, M. D. Zuluaga, and R. A. Houze, 2014: Severe convection and lightning in subtropical South America. *Geophys. Res. Lett.*, **41**, 7359–7366, https://doi.org/10.1002/2014GL061767.

——, M. M. Chaplin, M. D. Zuluaga, and R. A. Houze, 2016: Contribution of extreme convective storms to rainfall in South America. *J. Hydrometeor.*, **17**, 353–367, https://doi.org/10.1175/JHM-D-15-0067.1.

Rasmusson, E. M., and K. C. Mo, 1996: Large-scale atmospheric moisture cycling as evaluated from NMC global analysis and forecast products. *J. Climate*, **9**, 3276–3297, https://doi.org/10.1175/1520-0442(1996)009<3276:LSAMCA>2.0.CO;2.

Repinaldo, H. F. B., M. Nicolini, and Y. G. Skabar, 2015: Characterizing the diurnal cycle of low-level circulation and convergence using CFSR data in southeastern South America. *J. Appl. Meteor. Climatol.*, **54**, 671–690, https://doi.org/10.1175/JAMC-D-14-0114.1.

Rife, D. L., J. O. Pinto, A. J. Monaghan, C. A. Davis, and J. R. Hannan, 2010: Global distribution and characteristics of diurnally varying low-level jets. *J. Climate*, **23**, 5041–5064, https://doi.org/10.1175/2010JCLI3514.1.

Romatschke, U., and R. A. Houze, 2010: Extreme summer convection in South America. *J. Climate*, **23**, 3761–3791, https://doi.org/10.1175/2010JCLI3465.1.

Salio, P., M. Nicolini, and A. C. Saulo, 2002: Chaco low-level jet events characterization during the austral summer season. *J. Geophys. Res.*, **107**, 4816, https://doi.org/10.1029/2001JD001315.

——, ——, and E. J. Zipser, 2007: Mesoscale convective systems over southeastern South America and their relationship with the South American low-level jet. *Mon. Wea. Rev.*, **135**, 1290–1309, https://doi.org/10.1175/MWR3305.1.

Saulo, A. C., M. E. Seluchi, and M. Nicolini, 2004: A case study of a Chaco low-level jet event. *Mon. Wea. Rev.*, **132**, 2669–2683, https://doi.org/10.1175/MWR2815.1.

——, J. Ruiz, and Y. G. Skabar, 2007: Synergism between the low-level jet and organized convection at its exit region. *Mon. Wea. Rev.*, **135** 1310–1326, https://doi.org/10.1175/MWR3317.1.

Seluchi, M. E., A. C. Saulo, M. Nicolini, and P. Satyamurty, 2003: The northwestern Argentinean low: A study of two typical events. *Mon. Wea. Rev.*, **131**, 2361–2378, https://doi.org/10.1175/1520-0493(2003)131<2361:TNALAS>2.0.CO;2.

Servicio Meteorológico Nacional—Argentina, 2019: SMN radiosonde data, version 1.0. Accessed 26 September 2019, https://doi.org/10.26023/E8MP-0GD3-4903.

Shapiro, A., E. Fedorovich, and S. Rahimi, 2016: A unified theory for the Great Plains nocturnal low-level jet. *J. Atmos. Sci.*, **73**, 3037–3057, https://doi.org/10.1175/JAS-D-15-0307.1.

Silvers, L. G., and W. H. Schubert, 2012: A theory of topographically bound balanced motions and application to atmospheric low-level jets. *J. Atmos. Sci.*, **69**, 2878–2891, https://doi.org/10.1175/JAS-D-11-0309.1.

Stein, A. F., R. R. Draxler, G. D. Rolph, B. J. B. Stunder, M. D. Cohen, and F. Ngan, 2015: NOAA's hysplit atmospheric transport and dispersion modeling system. *Bull. Amer. Meteor. Soc.*, **96**, 2059–2077, https://doi.org/10.1175/BAMS-D-14-00110.1.

Stensrud, D. J., 1996: Importance of low-level jets to climate: A review. *J. Climate*, **9**, 1698–1711, https://doi.org/10.1175/1520-0442(1996)009<1698:IOLLJT>2.0.CO;2.

UCAR/NCAR–Earth Observing Laboratory, 2020: Multi-network composite highest resolution radiosonde data, version 1.3. Accessed 26 September 2019, https://doi.org/10.26023/GKFF-YNBJ-BV14.⟩

Uccellini, L. W., 1980: On the role of upper tropospheric jet streaks and leeside cyclogenesis in the development of low-level jets in the Great Plains. *Mon. Wea. Rev.*, **108**, 1689–1696, https://doi.org/10.1175/1520-0493(1980)108<1689:OTROUT>2.0.CO;2.

Velasco, I. Y., and J. M. Fritsch, 1987: Mesoscale convective complexes in the Americas. *J. Geophys. Res.*, **92**, 9591–9613, https://doi.org/10.1029/JD092iD08p09591.

Vera, C., and Coauthors, 2006: The South American low-level jet experiment. *Bull. Amer. Meteor. Soc.*, **87**, 63–78, https://doi.org/10.1175/BAMS-87-1-63.

Vila, D. A., L. A. T. Machado, H. Laurent, and I. Velasco, 2008: Forecast and tracking the evolution of cloud clusters (ForTraCC) using satellite infrared imagery: Methodology and validation. *Wea. Forecasting*, **23**, 233–245, https://doi.org/10.1175/2007WAF2006121.1.

Walters, C. K., J. A. Winkler, S. Husseini, R. Keeling, J. Nikolic, and S. Zhong, 2014: Low-level jets in the North American Regional Reanalysis (NARR): A comparison with rawinsonde observations. *J. Appl. Meteor. Climatol.*, **53**, 2093–2113, https://doi.org/10.1175/JAMC-D-13-0364.1.

Zipser, E. J., D. J. Cecil, C. Liu, S. W. Nesbitt, and D. P. Yorty, 2006: Where are the most intense thunderstorms on Earth? *Bull. Amer. Meteor. Soc.*, **87**, 1057–1071, https://doi.org/10.1175/BAMS-87-8-1057.